

## Supporting information

### Synthesis of a nanoscale Cu(II)<sub>31</sub>-oxo-carboxylate cluster, and effect of Cu-oxo cluster size on visible-light absorption

Thomas J. Barnes, Jack Payne, Sebastian D. Pike\*

#### Contents

Experimental Details	1
Synthetic Procedures	2
Supporting Figures	4
Bond Valence Sum Calculation Tables	23
Crystallography Data Tables	30
References	31

Associated datasets can be found at <http://wrap.warwick.ac.uk/171021/>

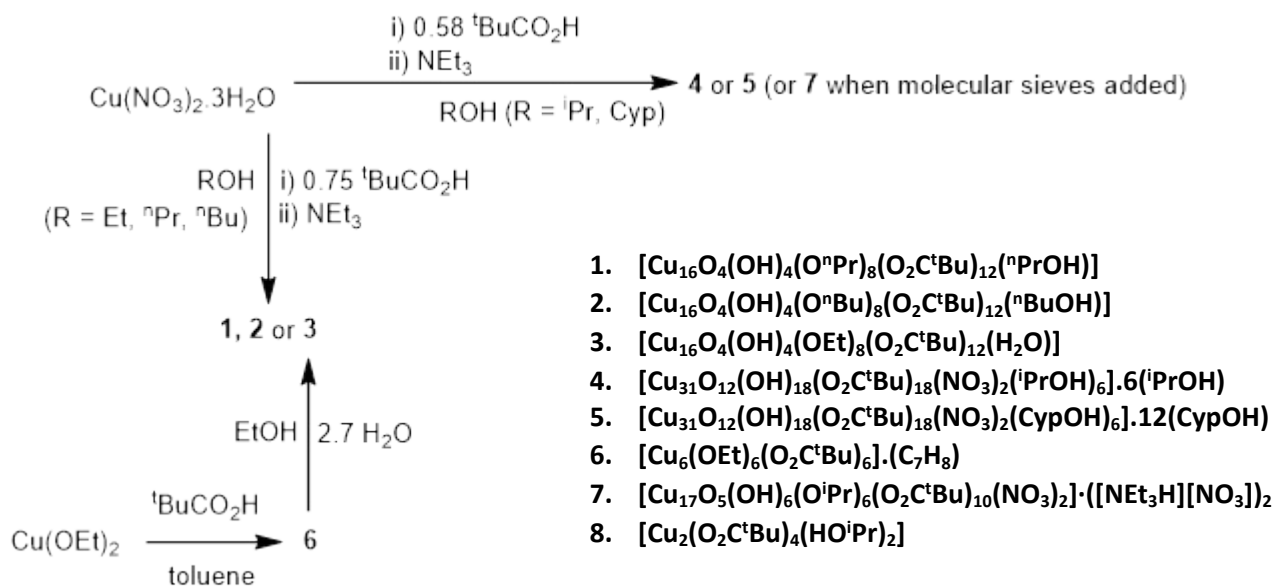
#### Experimental details

All reactions were performed at room temperature, under air unless otherwise stated. Oxygen or water sensitive reactions were performed under a nitrogen atmosphere using standard Schlenk line techniques. Dry solvents were either purchased in a dry form or dried *via* distillation, using CaH<sub>2</sub> (or Mg/I<sub>2</sub> for EtOH) as drying agent, and all were degassed by bubbling with N<sub>2</sub> and stored under N<sub>2</sub> over 4 Å molecular sieves (or 3 Å for alcohols). Reagents were purchased from Acros Organics (Cu(NO<sub>3</sub>)<sub>2</sub>·3H<sub>2</sub>O and LiOEt), Sigma Aldrich (Pivalic acid and NaO<sub>2</sub>C<sup>t</sup>Bu), Fischer Scientific (NEt<sub>3</sub>) and Alfa Aesar (CuCl<sub>2</sub>).

Powder X-ray diffraction (PXRD) patterns were measured on a Panalytical Empyrean with Cu source. Single crystal X-ray diffraction of **4** was carried out on a Bruker D8VENTURE equipped with high-brilliance I μScu-Kα radiation (1.54178 Å) (at 180K) Data integration and reduction were undertaken with SAINT and XPREP. Multi-scan empirical absorption corrections were applied to the data using SADABS.<sup>1</sup> Single crystal X-ray diffraction of other compounds was carried out with a Rigaku-Agilent Synergy diffractometer equipped with a HyPix-6000HE HPC detector, again with Cu-Kα radiation, at 100 K. All structures were solved ab initio using or Superflip<sup>2</sup> then refined with Crystals.<sup>3</sup> Crystallographic data have been deposited with the CCDC. Solution UV/Vis spectroscopy was carried out using an Implen C40 nanoPhotometer. Solid state UV/vis spectroscopy was carried out using a Shimadzu 2600i in diffuse reflectance mode with an integrating sphere attachment and was subtracted from a baseline of BaSO<sub>4</sub>. Elemental analysis was conducted on samples dried thoroughly under vacuum and was determined at London Metropolitan University by Orla McCullough. FTIR spectroscopy were conducted using an Agilent Technologies Cary 630 KBr FT-IR spectrometer with a Cary FTIR Diamond ATR accessory.

UV/vis spectra at varying concentrations were typically collected by serial dilution (50% dilution each step). Absorbance data was proportional to concentration consistent with the Beer Lambert rule. Where diluted solutions were used to calculate molar extinction coefficients the concentration was estimated by using the Beer Lambert rule with respect to the original (higher concentration) solution to reduce any propagating errors during serial dilution (**1**, estimated by serial dilution 0.015 mM, by Beer Lambert 0.023 mM; **2**, estimated by serial dilution 0.015 mM, by Beer Lambert 0.013 mM; **3**,

estimated by serial dilution 0.015 mM, by Beer Lambert 0.009 mM; **4**, estimated by serial dilution 0.0075 mM, by Beer Lambert 0.011 mM). This gave very good agreement in molar extinction values for the similar clusters **1-3**. Extinction values for **4** are given with  $\pm 33\%$  accuracy.



## Synthetic procedures

**Scheme S1.** Overview of synthetic routes to Compounds **1-7** and compound list.

### 1. $[\text{Cu}_{16}\text{O}_4(\text{OH})_4(\text{O}^n\text{Pr})_8(\text{O}_2\text{C}^t\text{Bu})_{12}(^n\text{PrOH})]$ , procedure optimised from Christou et al.<sup>4</sup>

$\text{Cu}(\text{NO}_3)_2 \cdot 3\text{H}_2\text{O}$  (1.0 g, 4.14 mmol) was dissolved in 50 mL of n-propanol. Pivalic acid (356  $\mu\text{L}$ , 3.10 mmol) was added to the solution.  $\text{NEt}_3$  (1.16 mL, 4.16 mmol) was added dropwise to the stirring solution, causing a colour change from blue to green. The solution was stirred for 30 minutes before sealing the flask and leaving it to sit for 24 hours. The solvent was then reduced to  $\sim 2$  mL and pentane ( $\sim 15$  mL) was added to precipitate  $[\text{NHEt}_3][\text{NO}_3]$ . The precipitate was discarded, and the solution placed at  $-20$   $^\circ\text{C}$  to yield green crystals (400 mg, 53%).

CHN analysis: Predicted ( $\text{Cu}_{16}\text{O}_4(\text{OH})_4(\text{O}^n\text{Pr})_8(\text{O}_2\text{C}^t\text{Bu})_{12}$ ) - C: 35.59%, H: 5.97%. Found - C: 35.58%, H: 5.84%. N.B. centrally bound  $^n\text{PrOH}$  neutral ligand not present by elemental analysis, this is likely removed by prolonged vacuum.

### 2. $[\text{Cu}_{16}\text{O}_4(\text{OH})_4(\text{O}^n\text{Bu})_8(\text{O}_2\text{C}^t\text{Bu})_{12}(^n\text{BuOH})]$ , procedure optimised from Christou et al.<sup>4</sup>

$\text{Cu}(\text{NO}_3)_2 \cdot 3\text{H}_2\text{O}$  (1.0 g, 4.14 mmol) was dissolved in 50 mL of n-butanol. Pivalic acid (356  $\mu\text{L}$ , 3.10 mmol) was added to the solution.  $\text{NEt}_3$  (1.16 mL, 4.16 mmol) was added dropwise to the stirring solution, causing a colour change from blue to green. The solution was stirred for 30 minutes before sealing the flask and leaving it to sit for 24 hours. The solvent was then reduced to  $\sim 2$  mL and pentane ( $\sim 15$  mL) was added to precipitate  $[\text{NHEt}_3][\text{NO}_3]$ . The precipitate was discarded, and the solution placed at  $-20$   $^\circ\text{C}$  to yield green crystals (423 mg, 53%).

CHN analysis: Predicted - C: 38.16%, H: 6.47%. Found - C: 38.12%, H: 6.39%.

### 3. $[\text{Cu}_{16}\text{O}_4(\text{OH})_4(\text{OEt})_8(\text{O}_2\text{C}^t\text{Bu})_{12}(\text{H}_2\text{O})]$

$\text{Cu}(\text{NO}_3)_2 \cdot 3\text{H}_2\text{O}$  (1.0 g, 4.14 mmol) was dissolved in 30 mL of ethanol. Pivalic acid (356  $\mu\text{L}$ , 3.10 mmol) was added to the solution.  $\text{NEt}_3$  (1.16 mL, 4.16 mmol) was added dropwise to the stirring solution, causing a colour change from blue to green. The solution was stirred for 30 minutes before sealing the flask and leaving to sit for three days to allow green solids to form. The solution was discarded, and the solids washed twice with ethanol. The remaining solids were dried under vacuum. 440 mg collected (62% yield).

CHN analysis: Predicted – C: 33.31%, H: 5.66%. Found – C: 32.72%, H: 5.31%.

### 4. $[\text{Cu}_{31}\text{O}_{12}(\text{OH})_{18}(\text{O}_2\text{C}^t\text{Bu})_{18}(\text{NO}_3)_2(\text{iPrOH})_6] \cdot 6(\text{iPrOH})$

$\text{Cu}(\text{NO}_3)_2 \cdot 3\text{H}_2\text{O}$  (1.0 g, 4.14 mmol) was dissolved in 200 mL of isopropanol. Pivalic acid (276  $\mu\text{L}$ , 2.4 mmol) was added to the solution.  $\text{NEt}_3$  (1.7 mL, 12.2 mmol) was added dropwise to the stirring solution, causing a colour change from blue to green. The solution was stirred for 30 minutes before sealing the flask and leaving it to sit in the dark for two weeks to allow crystalline material to form. The solution was discarded and the solids isolated (72 mg, 11%).

CHN analysis: Predicted  $\text{Cu}_{31}\text{O}_{12}(\text{OH})_{18}(\text{O}_2\text{C}^t\text{Bu})_{18}(\text{NO}_3)_2(\text{iPrOH})_6 \cdot 4(\text{iPrOH})$  – C: 28.75%, H: 5.23%, N: 0.56%. Found – C: 28.65%, H: 5.23%, N: 0.58%. N.B. two molecules of co-crystallised  $\text{iPrOH}$  solvent appear to be lost under prolonged vacuum.

### 5. $[\text{Cu}_{31}\text{O}_{12}(\text{OH})_{18}(\text{O}_2\text{C}^t\text{Bu})_{18}(\text{NO}_3)_2(\text{CypOH})_6] \cdot 12(\text{CypOH})$

250 mg (1.03 mmol) of  $\text{Cu}(\text{NO}_3)_2 \cdot 3\text{H}_2\text{O}$  was dissolved in 7.5 mL cyclopentanol in a round bottomed flask. To this 89  $\mu\text{L}$  (0.77 mmol) of pivalic acid was added whilst stirring. After 30 minutes stirring, 290  $\mu\text{L}$  (2.06 mmol) of  $\text{NEt}_3$  was added to give a green solution. This was sealed and left in a dark place for two weeks to yield a small quantity of crystals of **6** on the walls of the flask, which were characterised by single-crystal X-ray diffraction only.

### 6. $[\text{Cu}_6(\text{OEt})_6(\text{O}_2\text{C}^t\text{Bu})_6] \cdot (\text{C}_7\text{H}_8)$

$\text{Cu}(\text{OEt})_2$  was prepared from  $\text{CuCl}_2$  and  $\text{LiOEt}$  by literature routes.<sup>5</sup>  $\text{Cu}(\text{OEt})_2$  (0.5 g, 3.25 mmol) was suspended in dry toluene (70 mL) under a nitrogen atmosphere. Pivalic acid (374  $\mu\text{L}$ , 3.25 mmol) was added and the reaction stirred at 70 °C for 24 hours, producing a dark blue precipitate and a green solution. The solution was discarded, and the solids dried under vacuum to give **6** as a dark blue crystalline solid (300 mg, 50% yield).

CHN analysis: Predicted  $[\text{Cu}_6(\text{OEt})_6(\text{O}_2\text{C}^t\text{Bu})_6] \cdot (\text{C}_7\text{H}_8)_{0.7}$  – C: 42.58%, H: 6.83%. Found – C: 42.56%, H: 6.73%. N.B. partial removal of co-crystallised toluene occurs under prolonged vacuum.

### 7. $[\text{Cu}_{17}\text{O}_5(\text{OH})_6(\text{O}^i\text{Pr})_6(\text{O}_2\text{C}^t\text{Bu})_{10}(\text{NO}_3)_2] \cdot ([\text{NEt}_3\text{H}][\text{NO}_3])_2$

$\text{Cu}(\text{NO}_3)_2 \cdot 3\text{H}_2\text{O}$  (0.5 g, 2.06 mmol) was dissolved in 30 mL of isopropanol. Pivalic acid (138  $\mu\text{L}$ , 1.20 mmol) was added to the solution.  $\text{NEt}_3$  (575  $\mu\text{L}$ , 4.14 mmol) was added dropwise to the stirring solution, causing a colour change from blue to green. The solution was stirred for 30 minutes before 3 Å molecular sieves (~10 g) were added and the solution was degassed by bubbling with  $\text{N}_2$  gas. The

flask was sealed under a nitrogen atmosphere and left in the dark. Crystals of **7** formed on the side of the flask after one month (54 mg isolated, 14% yield).

CHN analysis: Predicted – C: 31.19%, H: 5.56%, N: 2.73%. Found – C: 30.52%, H: 5.16%, N: 2.62%

#### 8. $[\text{Cu}_2(\text{O}_2\text{C}^t\text{Bu})_4(\text{}^i\text{PrOH})_2] \cdot [\text{Cu}_2(\text{O}_2\text{C}^t\text{Bu})_4(\text{H}_2\text{O})_2] \cdot (\text{}^i\text{PrOH})_2$

A similar preparation was used as for previously reported Cu-pivalate paddlewheel compounds.<sup>6</sup> 1 g (4.14 mmol) of  $\text{Cu}(\text{NO}_3) \cdot 3\text{H}_2\text{O}$  and 1.2 g (8.28 mmol)  $\text{Na}(\text{O}_2\text{C}^t\text{Bu})$  were added to 30 mL isopropanol. The resulting suspension was stirred at room temperature for 30 minutes, and filtered. The solution was then dried to a turquoise solid under vacuum which was recrystallised from DCM at  $-20^\circ\text{C}$  to give a microcrystalline compound (251 mg, 19% yield). The crystalline compound was found to exist as a co-crystallisation of  $[\text{Cu}_2(\text{O}_2\text{C}^t\text{Bu})_4(\text{}^i\text{PrOH})_2]$  and  $[\text{Cu}_2(\text{O}_2\text{C}^t\text{Bu})_4(\text{H}_2\text{O})_2]$  with two isopropanol solvent molecules which coordinate through H-bonding. The two clusters vary only in the terminal ligands ( ${}^i\text{PrOH}$  or  $\text{H}_2\text{O}$ ), it is expected that these ligands are in dynamic exchange in solution.

CHN analysis: Predicted  $[\text{Cu}_2(\text{O}_2\text{C}^t\text{Bu})_4(\text{HO}^i\text{Pr})_2] \cdot [\text{Cu}_2(\text{O}_2\text{C}^t\text{Bu})_4(\text{H}_2\text{O})_2]$  – C: 45.31%, 7.61%. Found – C: 45.26%, H: 6.73%. N.B. co-crystallised isopropanol molecules likely lost under elongated vacuum.

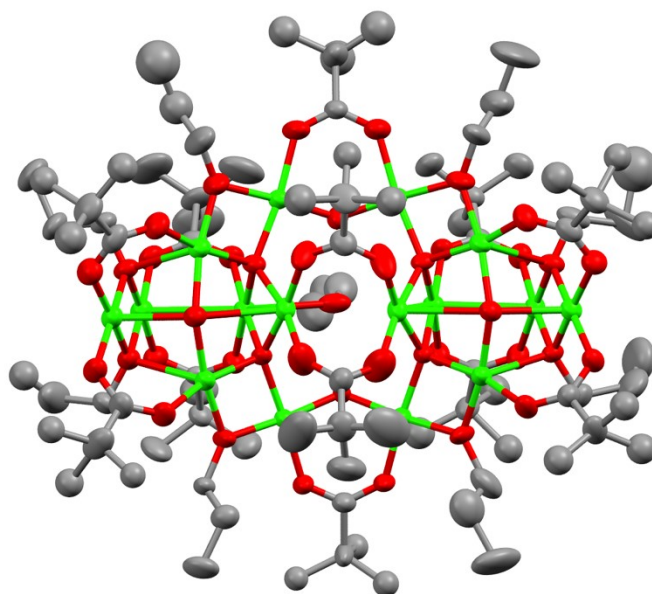


**Figure S1:** X-ray crystal structure of **1** (data taken from Christou et al.<sup>4</sup>) Green = Cu, Red = O, Grey = C. Ellipsoids displayed at 50% and hydrogens omitted for clarity.

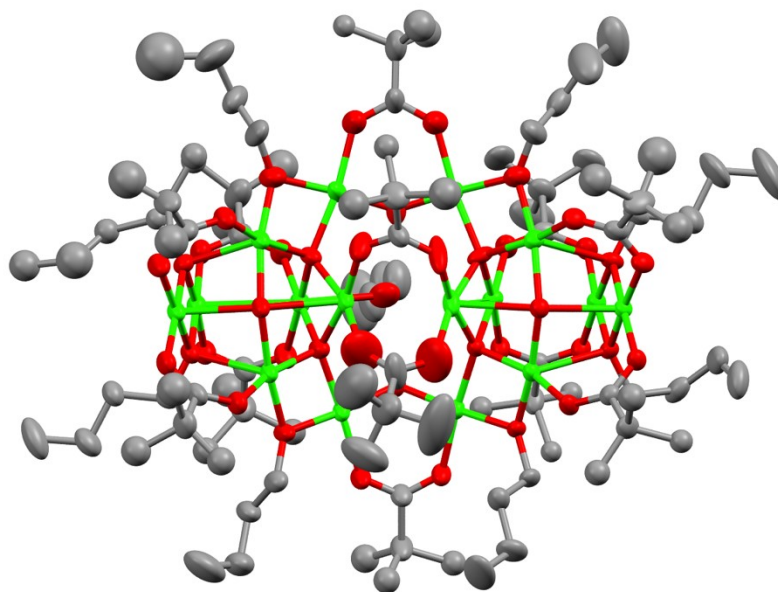


**Figure S2:** X-ray crystal structure of **2** (data taken from Christou et al.<sup>1</sup>). Green = Cu, Red = O, Grey = C. Ellipsoids displayed at 50% and hydrogens omitted for clarity.

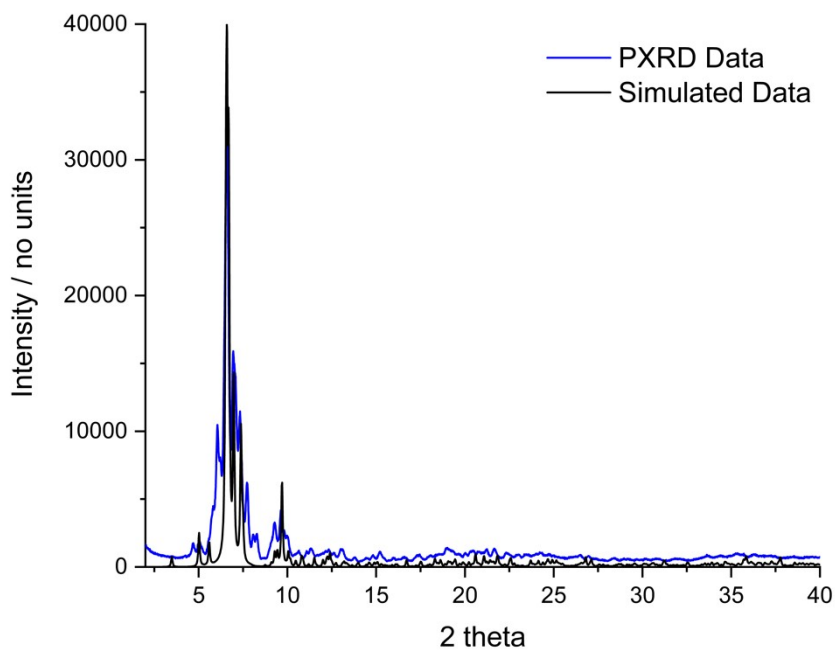


**Figure S3:** Powder X-ray diffraction pattern of a bulk sample of **2**.

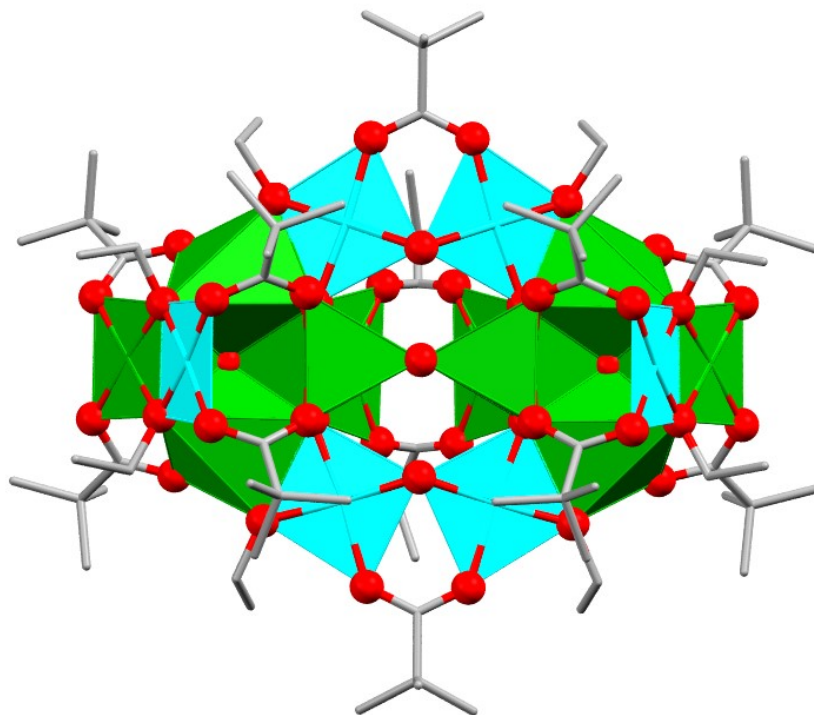


**Figure S4:** X-ray crystal structure of **3** shown in polyhedron view. Cyan = 4-coordinate Cu, Green = 5-coordinate Cu, Red = O, Grey = C. Ellipsoids displayed at 50% and hydrogens omitted for clarity.

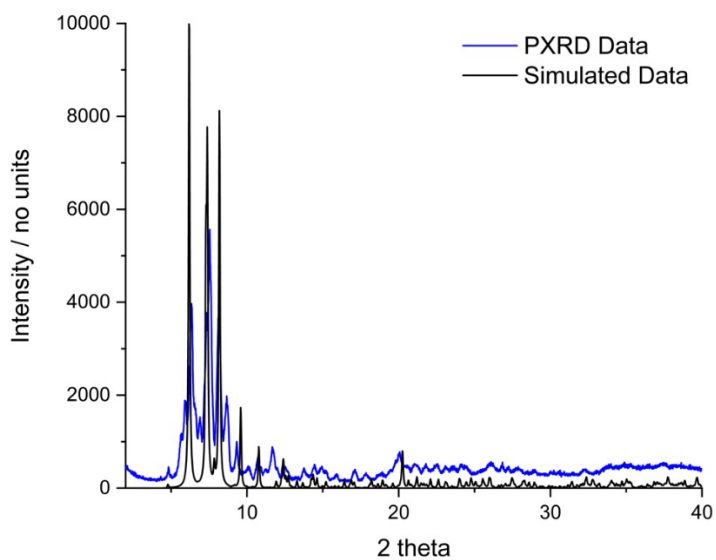


**Figure S5:** Powder X-ray diffraction pattern of a bulk sample of **3**.

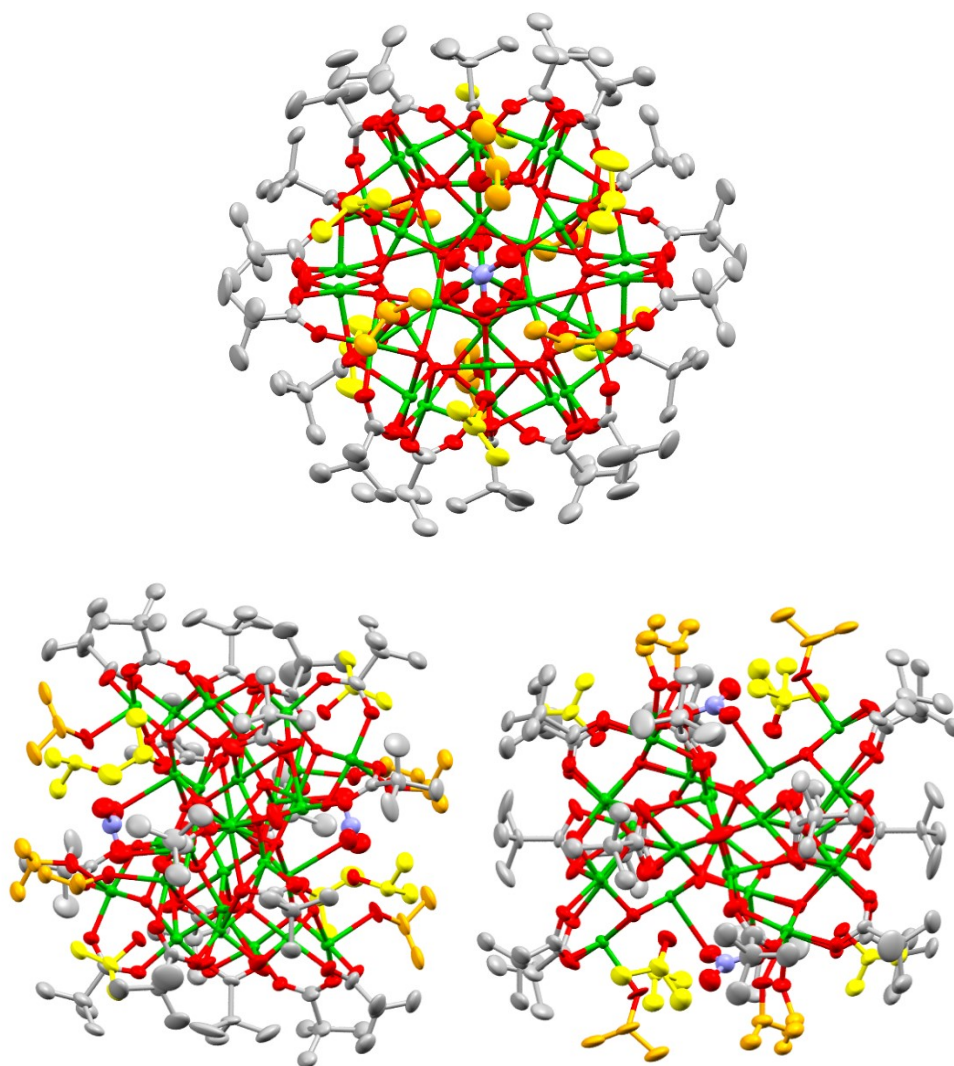


**Figure S6:** X-ray crystal structure of **4** from three angles. Green = Cu, Light blue = N, Red = O, Grey = C (non-coordinated/H-bonded <sup>i</sup>PrOH Cs shown in yellow, coordinated <sup>i</sup>PrOH Cs shown in orange). Ellipsoids displayed at 50% and hydrogens omitted for clarity.



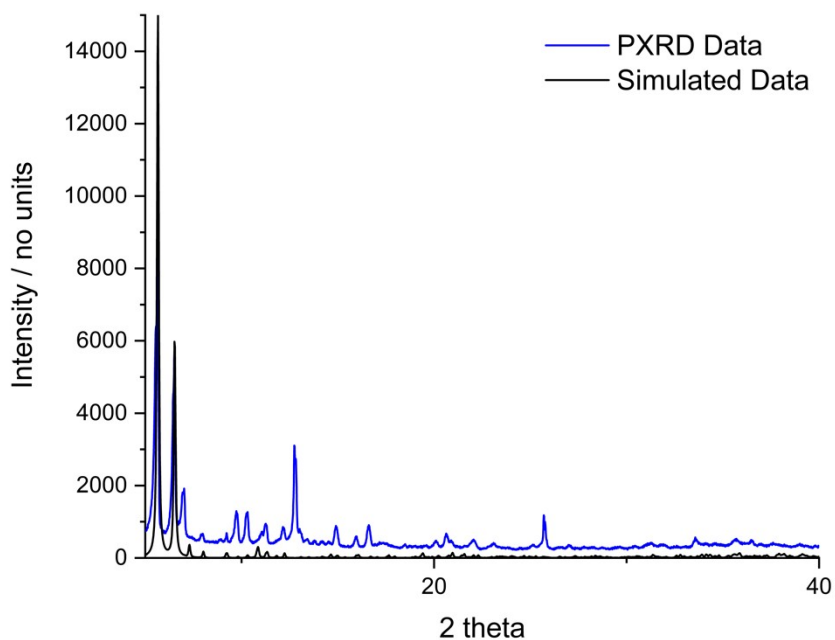


**Figure S7:** Powder X-ray diffraction pattern of a bulk sample of **4**. Minor impurities are identified by the sharp peaks at  $2\theta = 12.8$  and  $25.8^\circ$  from a  $\text{Cu}_2(\text{OH})_3(\text{NO}_3)$ ,<sup>7</sup> and other minor peaks are consistent with small amount of paddlewheel by-product  $\text{Cu}_2(\text{O}_2\text{C}^t\text{Bu})_4(\text{NEt})_3$ .<sup>8</sup>

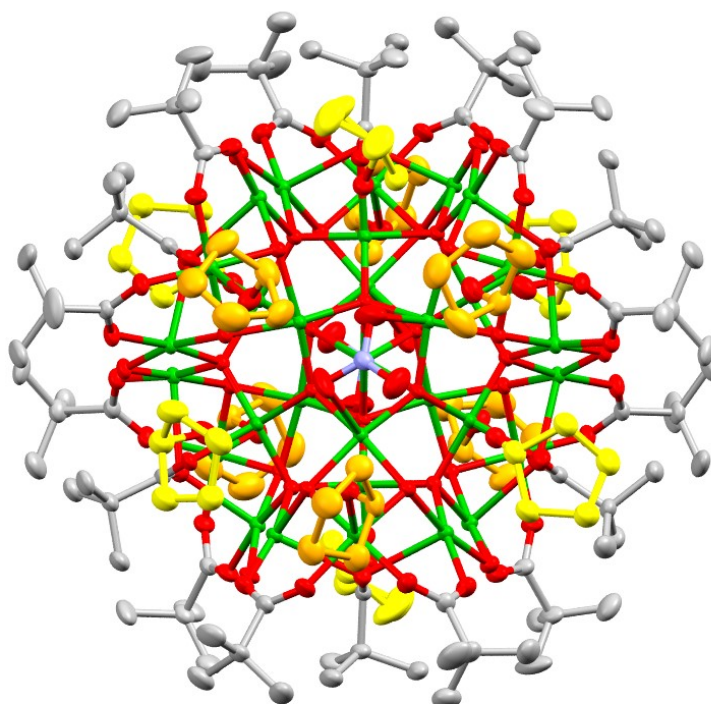


**Figure S8:** X-ray crystal structure of **5**. Green = Cu, Light blue = N, Red = O, Grey = C (non-coordinated/H-bonded *i*PrOH Cs shown in yellow, coordinated *i*PrOH Cs shown in orange). Ellipsoids displayed at 50% and hydrogens and 6 non-coordinated CypOH solvent molecules omitted for clarity.



**Supporting note 1.** **4** and **5** contain a combination of four and five coordinate Cu centres and a single octahedral site at the centre. The 16 crystallographically separate Cu sites can be grouped into 3 'corner' sites, 6 'edge' sites, 3 'mid' sites, 3 'nitrate' and the central octahedral site (Fig S10, below). Most sites adopt an approximately square based pyramidal 5-coordinate geometry with variable bond lengths to the apical position. The 'mid' sites have a longer bond within the square plane and a shorter bond angled above the square plane, both Os arising from the same carboxylate in a slipped chelate mode.

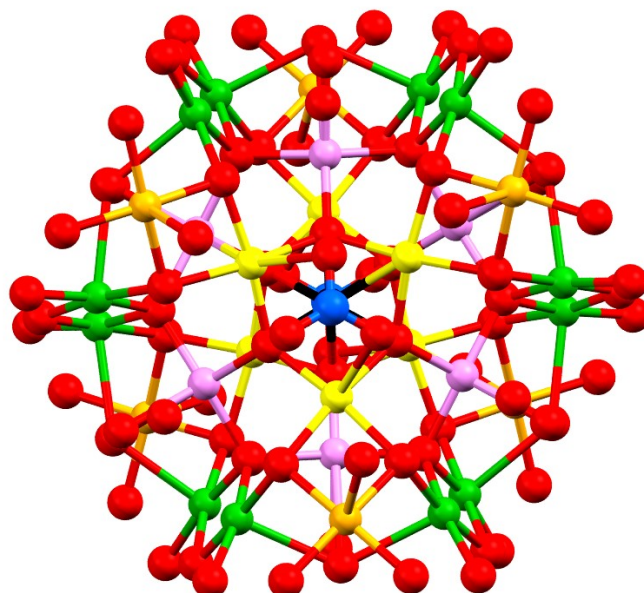


**Figure S9.** X-ray structure of the Cu-O core of **4** with similar Cu sites grouped by colour. 'Corner' sites = orange, 'edge' sites = green, 'mid' sites = violet, 'nitrate' = yellow and the central octahedral site = black.

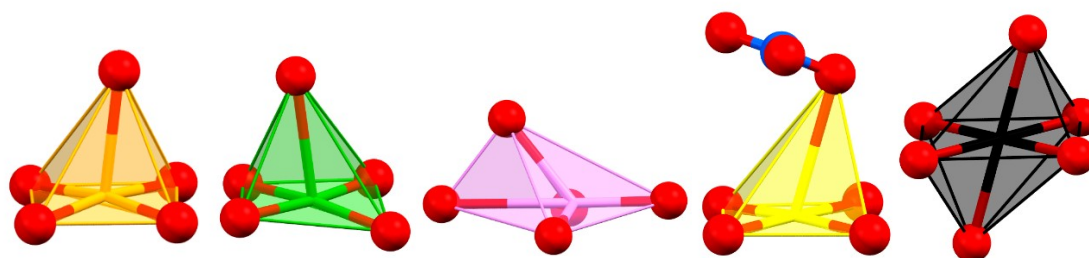


**Figure S10.** Polyhedron view of a 'corner' site = orange, 'edge' site = green, 'mid' site = violet, 'nitrate' site = yellow and the central octahedral site = black.

**Table S1.** Geometries of Cu centres with Cu–O bond lengths (Cu labels taken from crystal structure of **4**, with equivalent positions reported in the same column for **5**). Range of bond lengths to four Os in approximate square plane given, with *bond-length to apical O given in italics in the case of 5-coordinate centres*. Bonds beyond 2.8 Å greyed (N.B. sum of van der waals radii = 2.92 Å). Where apical site is significantly away from centre of square plane ‘angled’ is noted.

Cu label and description	<b>4</b> Cu–O bond lengths (Å)	<b>5</b> Cu–O bond lengths (Å)
1 corner	1.93-1.99 + 2.35 (+ 2.85)	1.93-1.98 + 2.30
2 nitrate	1.92-2.02 + 2.77	1.89-2.01 + 2.62
3 nitrate	1.89-2.01 + 2.71	1.92-2.01
4 edge	1.91-2.00 + 2.47	1.92-1.98 + 2.52
5 centre	Octahedral 2.02-2.22	Octahedral 1.98-2.37
6 nitrate	1.92-2.03 + 2.89	1.90-2.04 + 2.74
7 mid	1.90-2.80 (+ 2.11 angled)	1.90-2.83 (+ 2.06 angled)
8 edge	1.92-1.98 + 2.44	1.92-2.00 + 2.38
9 mid	1.90-2.58 + 2.19 angled	1.91-2.28 + 2.35 angled
10 corner	1.93-1.99 + 2.31	1.93-1.98 + 2.29
11 edge	1.91-2.01 + 2.43	1.91-2.00 + 2.48
12 edge	1.88-1.98 + 2.47	1.92-1.99 + 2.44
13 mid	1.90-2.66 + 2.16 angled	1.89-2.83 + 2.08 angled
14 corner	1.94-1.99 + 2.31 (+2.84)	1.93-2.00 + 2.29 (+ 2.81)
15 edge	1.89-1.95 + 2.47	1.92-2.00 + 2.40
16 edge	1.91-2.00 + 2.43	1.92-2.00 + 2.49

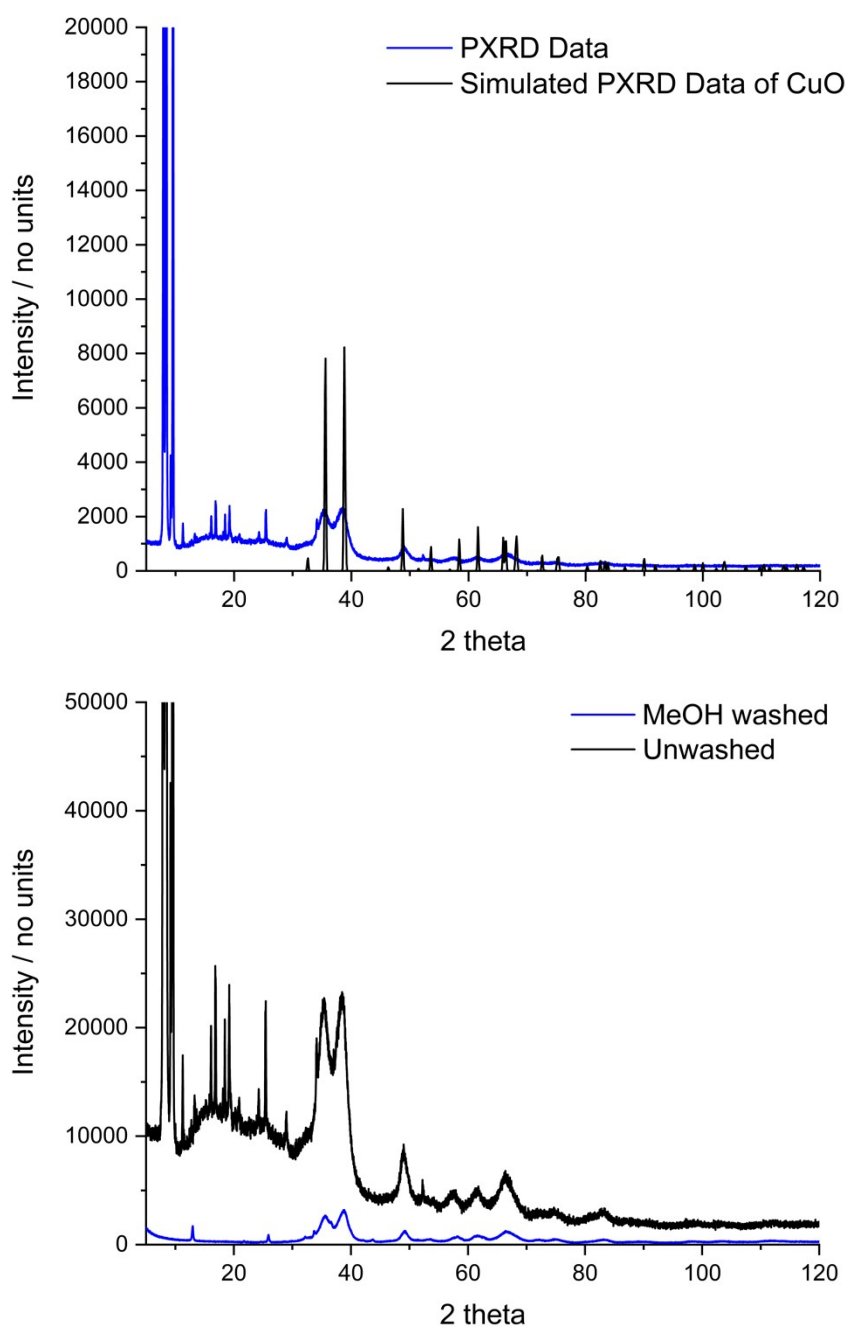


**Figure S11:** Powder X-ray diffraction patterns of the brown precipitate that formed after 2 weeks in a reaction targeting **4** but that was left open to air. Top pattern shows the crude product against the expected pattern for bulk CuO (data from Greaves et al, collection code 133363)<sup>9</sup>. The product contains CuO nanoparticles and unidentified molecular species (low angle peaks). Scherrer analysis of the reflections at  $2\theta = 35^\circ$  and  $38^\circ$  gives estimated crystallite diameters of 8 and 15 nm. The bottom patterns show the PXRD pattern before and after washing the crude product with MeOH. A small trace of  $\text{Cu}_2(\text{OH})_3(\text{NO}_3)$  is also noted in both spectra (peaks at  $2\theta = 12.8$  and  $25.8^\circ$ ).<sup>7</sup>

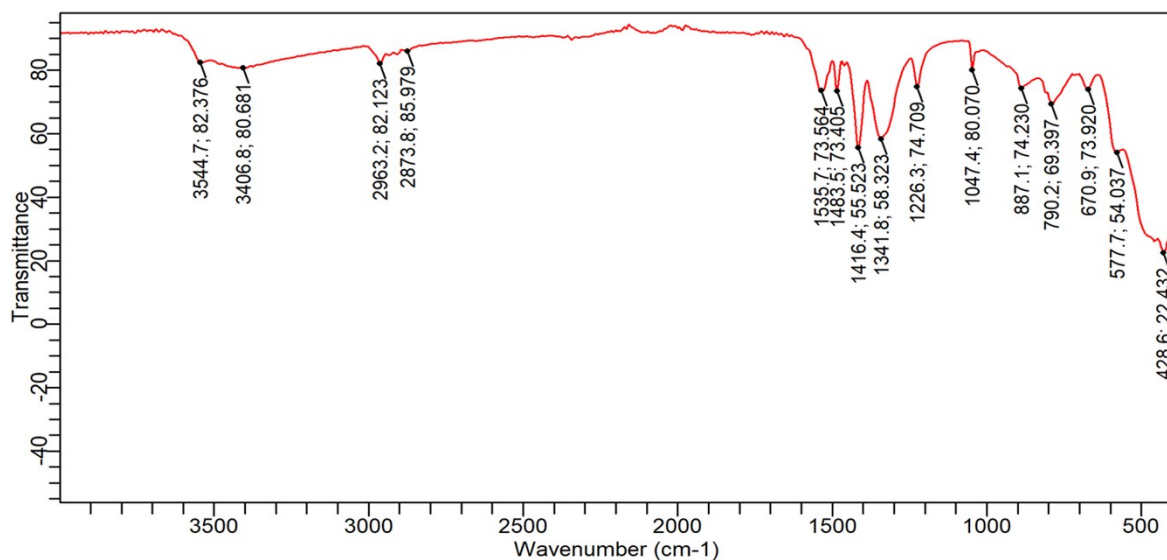


**Figure S12.** FTIR spectrum of the brown precipitate (containing CuO nanoparticles) that formed after two weeks in a reaction targeting **4** but that was left open to air. The sample was washed with MeOH before collecting the spectrum. Sample shows C–H (2963  $\text{cm}^{-1}$ ) and O=C–O (1536 and 1416  $\text{cm}^{-1}$ ) stretches expected for pivalate capping the CuO nanoparticle surfaces.<sup>10</sup>

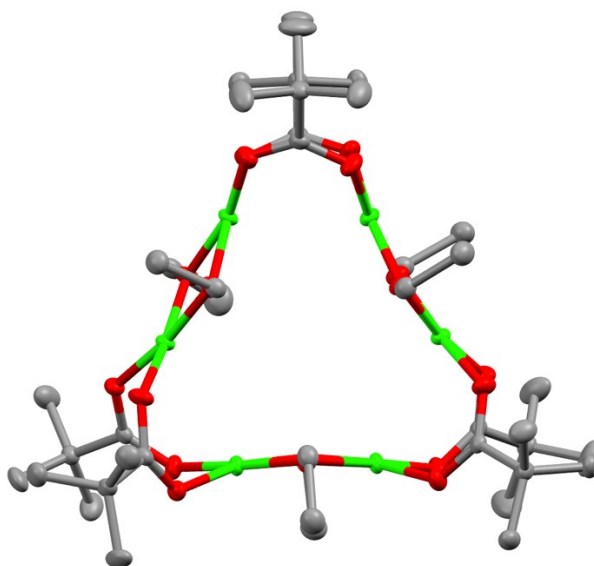


**Figure S13:** X-ray crystal structure of **6**. Green = Cu, Red = O, Grey = C. Ellipsoids displayed at 50% and hydrogens omitted for clarity.

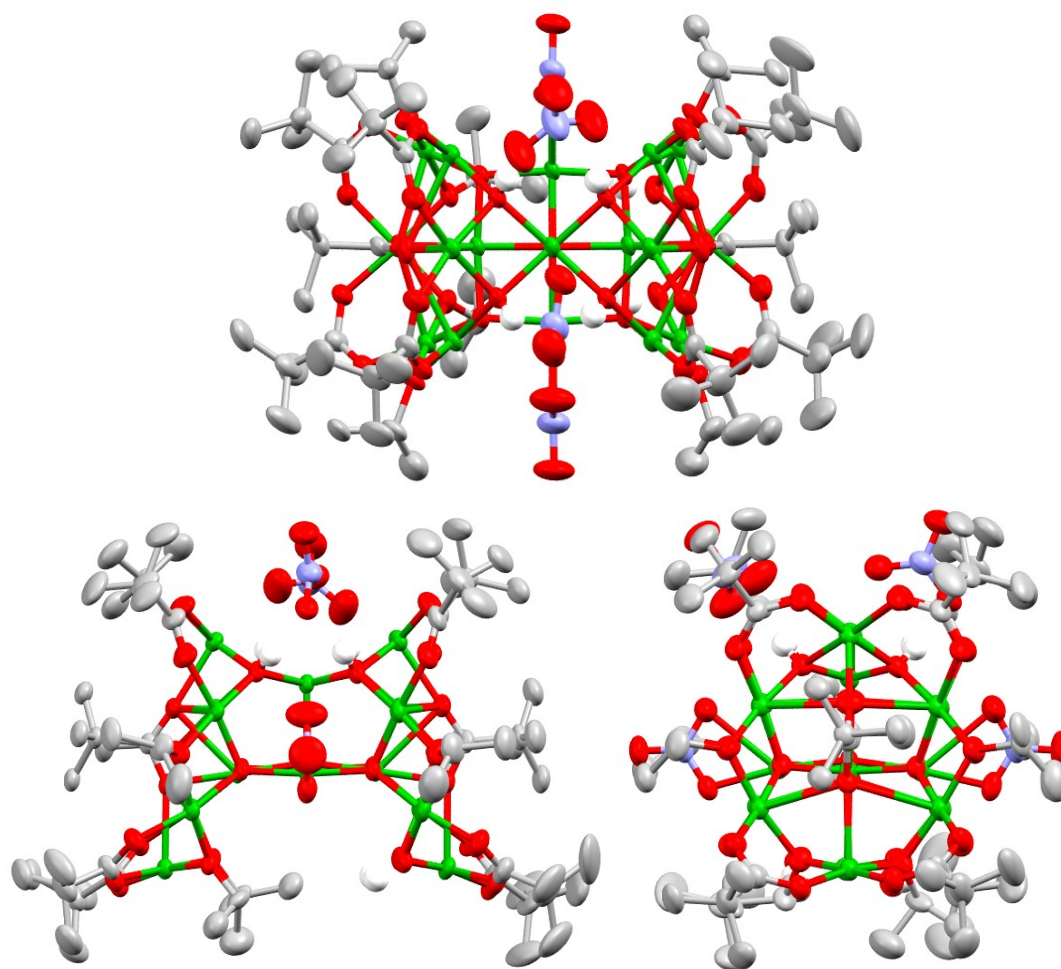


**Figure S14:** X-ray crystal structure of **7** from three different angles. Green = Cu, Light blue = N, Red = O, Grey = C, White = H. Ellipsoids displayed at 50% and hydrogens (except OH groups) and  $[\text{NEt}_3\text{H}]^+$  cations omitted for clarity.

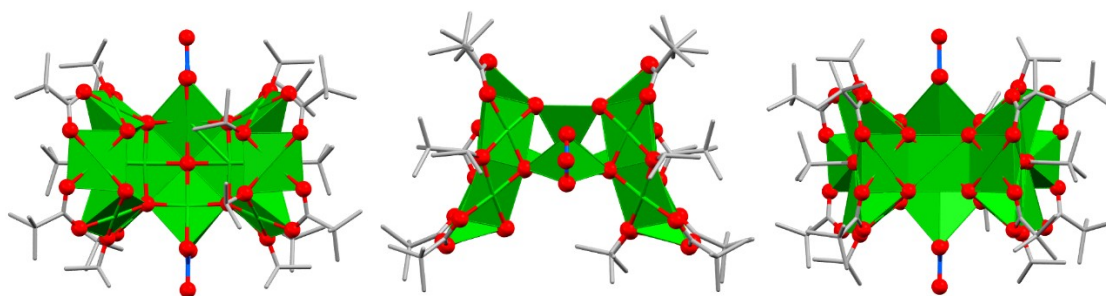


**Figure S15.** Polyhedron view of the X-ray structure of **7** from three different angles.

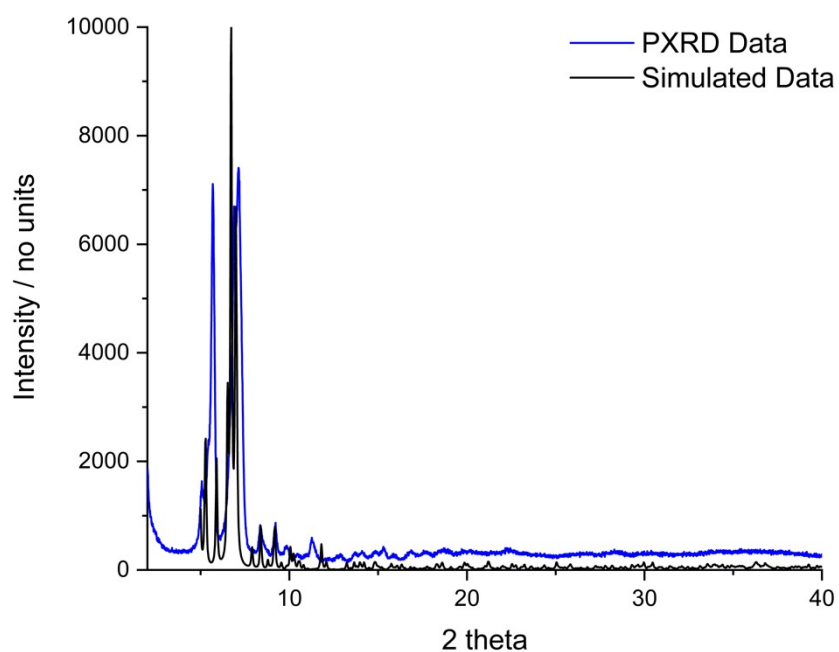


**Figure S16:** Powder X-ray diffraction pattern of a bulk sample of **7**.

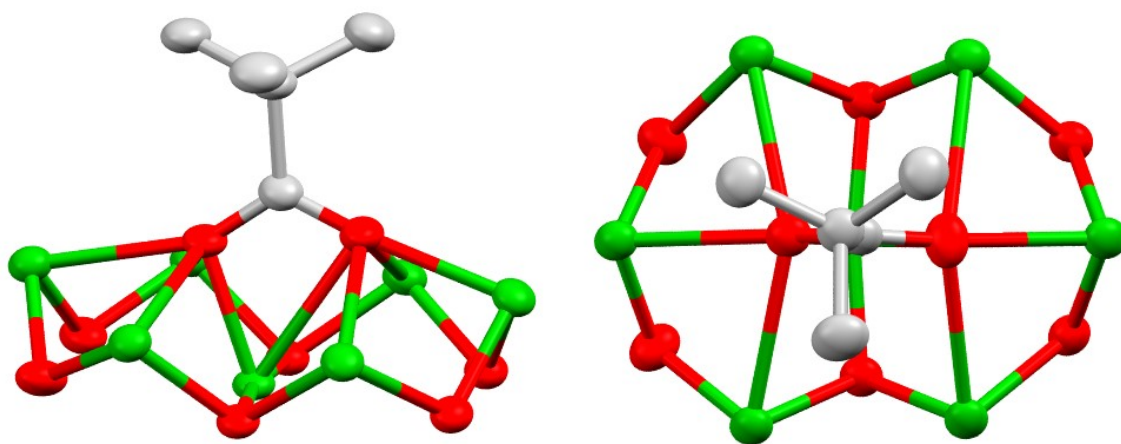


**Figure S17:** X-ray structure extract of seven coordinating pivalate anion in **7** Green = Cu, Light blue = N, Red = O, Grey = C. Ellipsoids displayed at 50% and hydrogens omitted for clarity. Carboxylate(O)–Cu bond length range 2.074(3)–2.777(3) Å.

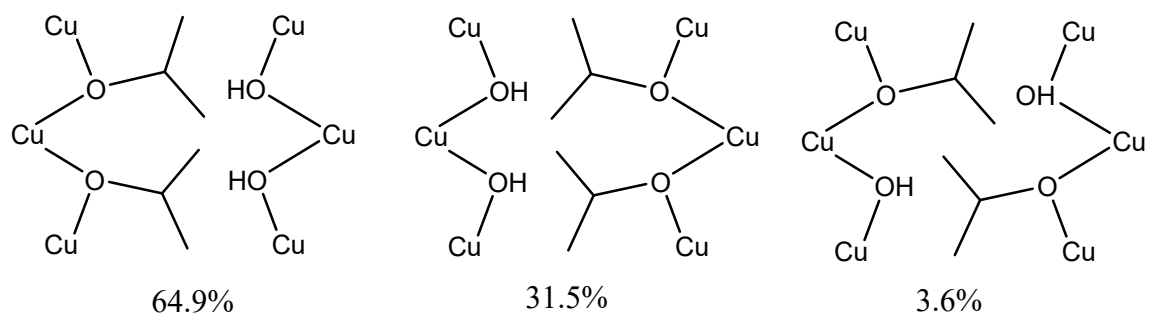


**Figure S18.** The internal cleft of **7** contains disordered O<sup>i</sup>Pr/OH moieties over four sites. Based on refining the occupancy of the carbon atoms (including disorder over two sites at each position) the disorder model shown here was used.



**Figure S19:** Photos showing, from left to right, CH<sub>2</sub>Cl<sub>2</sub> solutions of **8**, **6**, **2**, **7** and **4**. All at [Cu] ~ 0.24 mM (except for **7** which is approximately [Cu] ~ 0.48 mM)



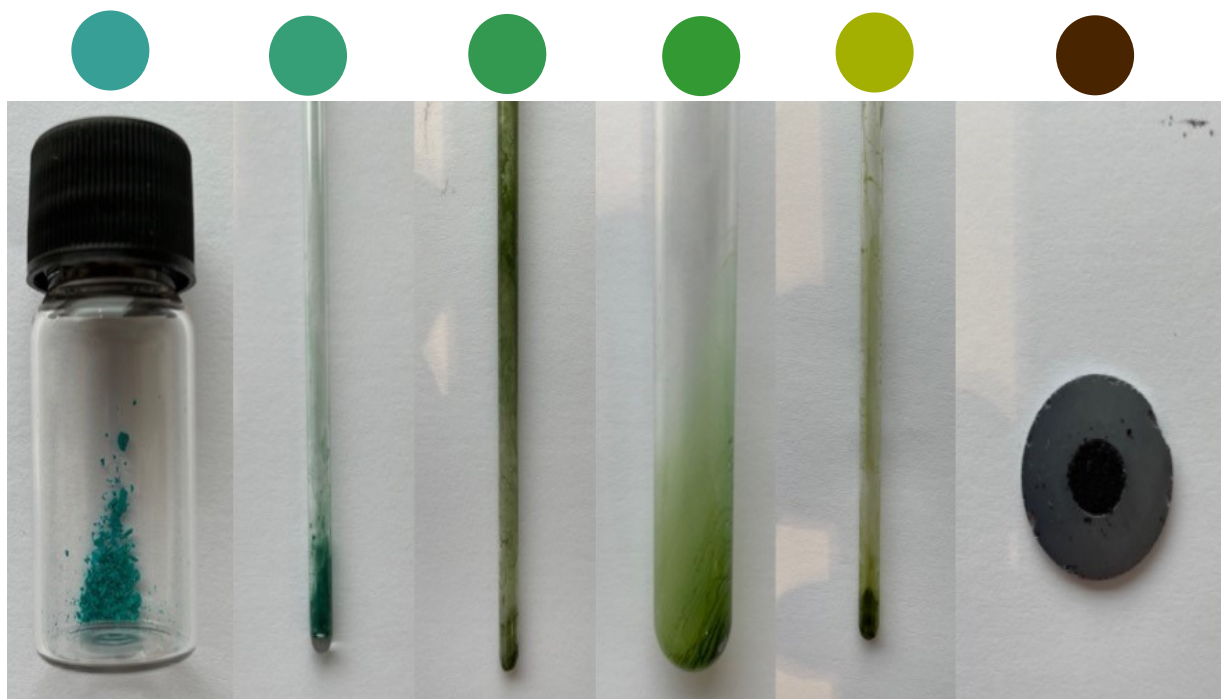


**Figure S20:** Solid state pictures of (from left to right) **8**, **6**, **2**, **7**, **4** and CuO nanoparticles. All colours as solids resemble the colours of solutions, except for **8** which appears a much deeper blue when dissolved.

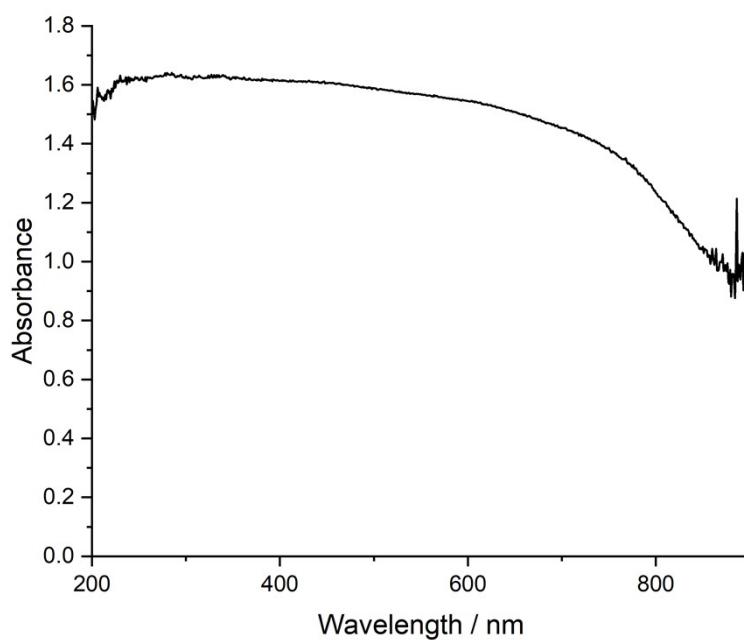


**Figure S21.** Diffuse-reflectance solid-state UV/visible spectrum of the dark brown precipitate (containing CuO nanoparticles) that formed after two weeks in a reaction targeting **4** but that was

left open to air. The precipitate was washed with MeOH before collecting this spectrum. The spectrum shows strong absorbance across the UV and visible region.

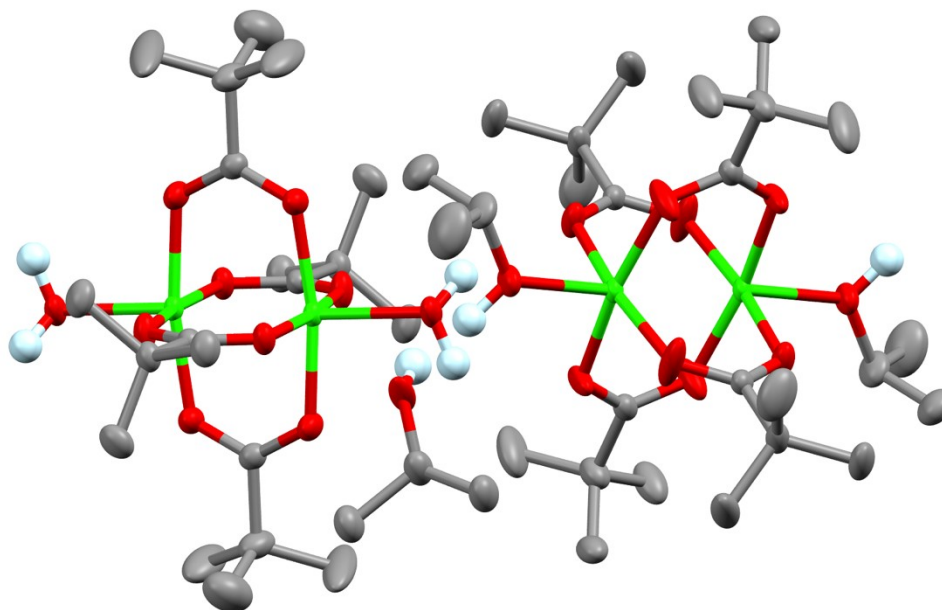


**Figure S22.** X-ray crystal structure of **8**. This paddlewheel structure crystallises as a co-crystal of two structures; one containing coordinated water ligands and one with coordinated *i*PrOH ligands. Two *i*PrOH solvent molecules form hydrogen bonding network between the coordinated water and *i*PrOH groups on the two paddlewheel structures. Green = Cu, Red = O, Grey = C, Light blue = H. Ellipsoids displayed at 50% and hydrogens (except those involved in hydrogen bonding) omitted for clarity.

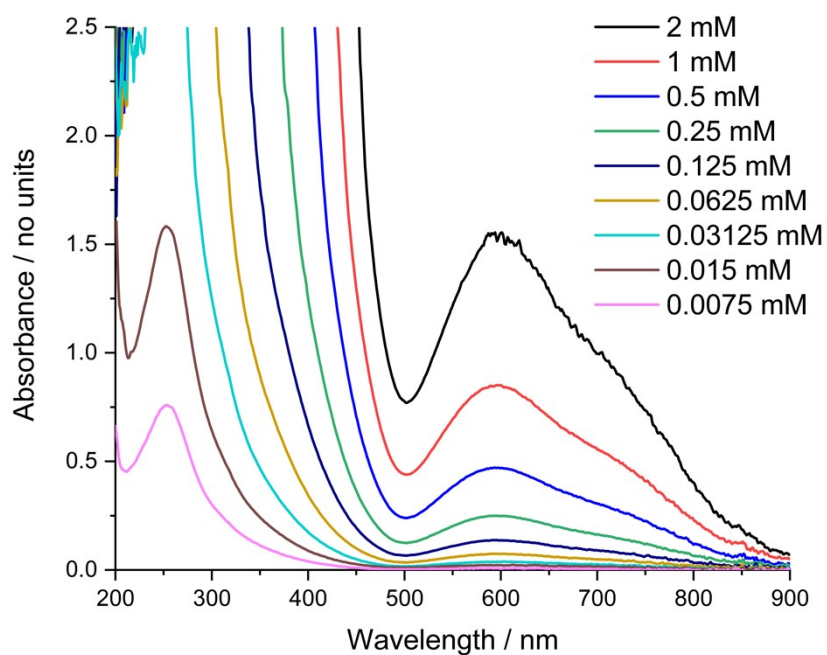


**Figure S23:** UV/vis spectrum of **1** at varying molecular concentrations in pentane. Serial dilutions consistent with Beer-Lambert law. However, due to slight inaccuracy of serial dilutions estimated concentrations are likely closer to (2, 1.1, 0.62, 0.32, 0.17, 0.09, 0.05, 0.023, 0.011 mM).

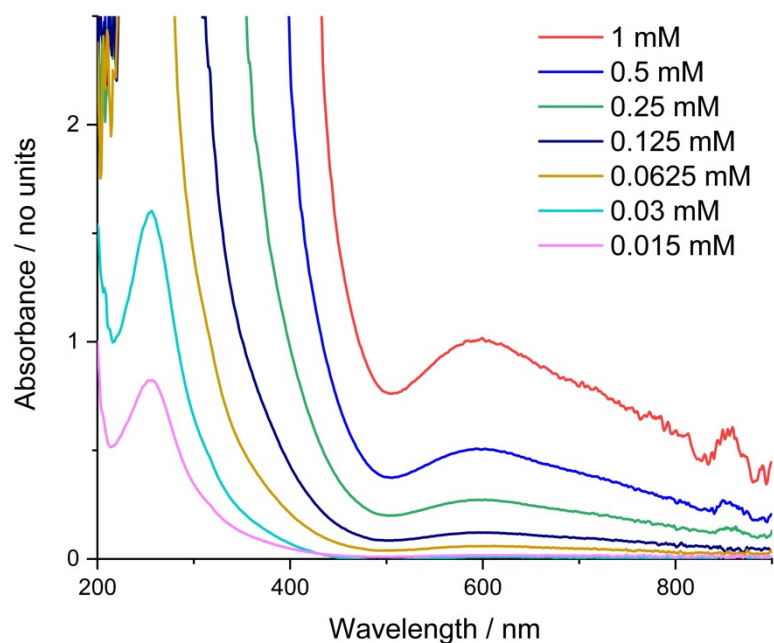


**Figure S24:** UV/vis spectrum of **2** at varying molecular concentrations in pentane. Serial dilutions consistent with Beer-Lambert law.

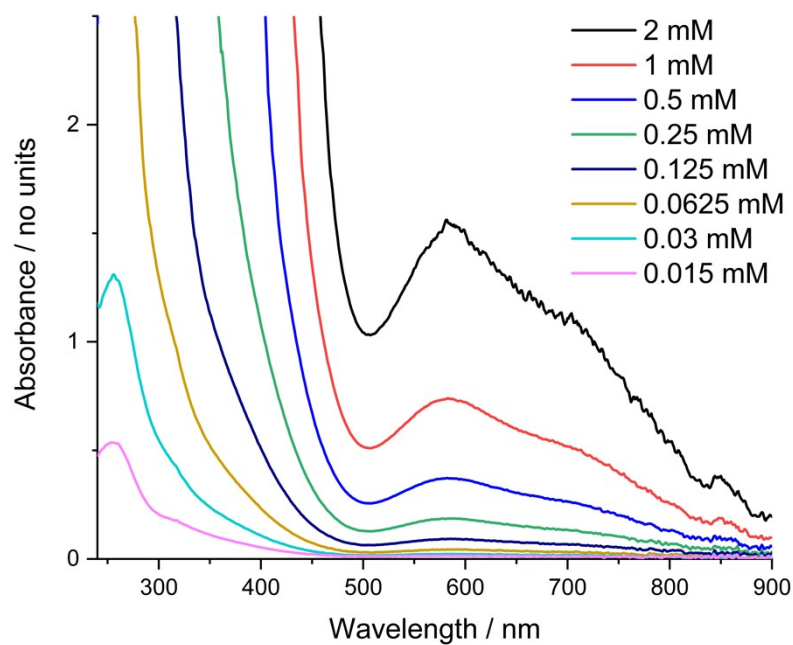


**Figure S25:** UV/vis spectrum of **3** at varying molecular concentrations in  $\text{CH}_2\text{Cl}_2$ . Serial dilutions consistent with Beer-Lambert law.

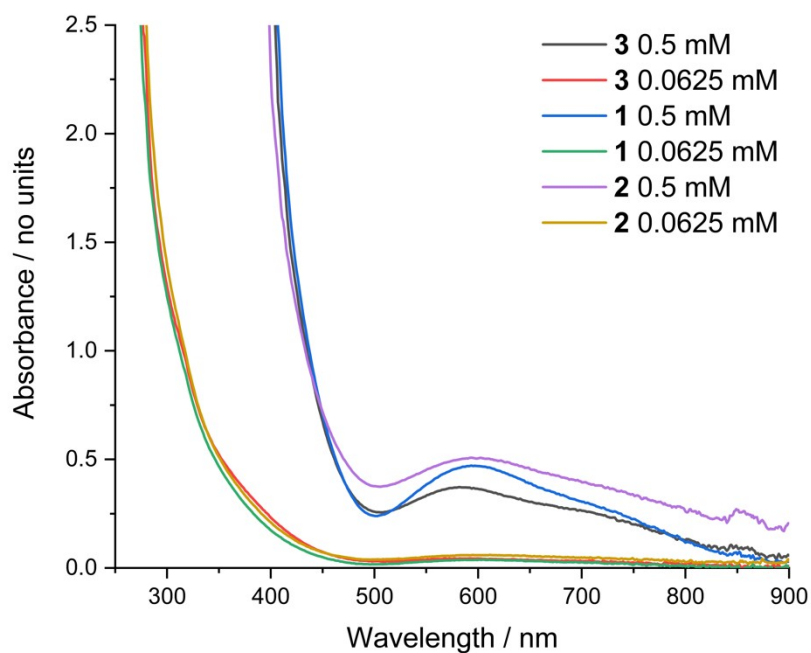


**Figure S26:** UV/vis spectrum of **1**, **2** and **3** at two different concentrations (dissolved in pentane for **1** and **2** and  $\text{CH}_2\text{Cl}_2$  **3**). The differences in the spectra in the d-d region may be explained from slightly different Cu(II) geometries found in the different  $\text{Cu}_{16}$  structures.

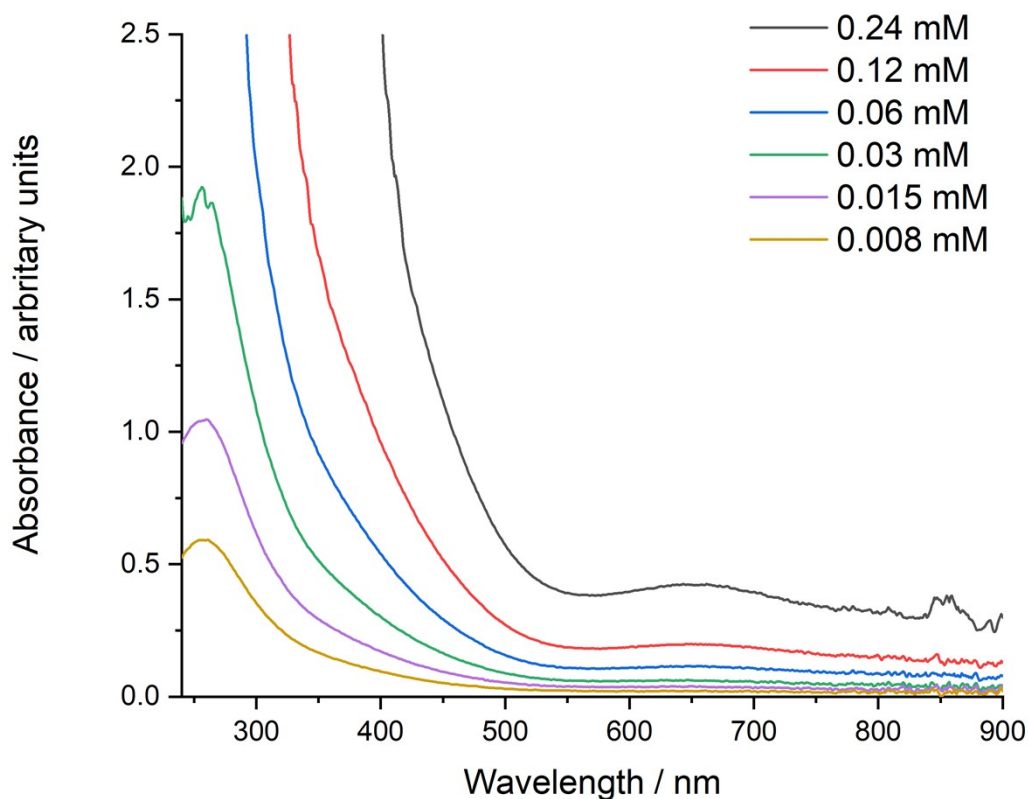


**Figure S27:** UV/vis spectrum of **4** at varying compound concentrations in  $\text{CH}_2\text{Cl}_2$ . Serial dilutions consistent with Beer-Lambert law. Concentrations given with an error of  $\pm 33\%$ .

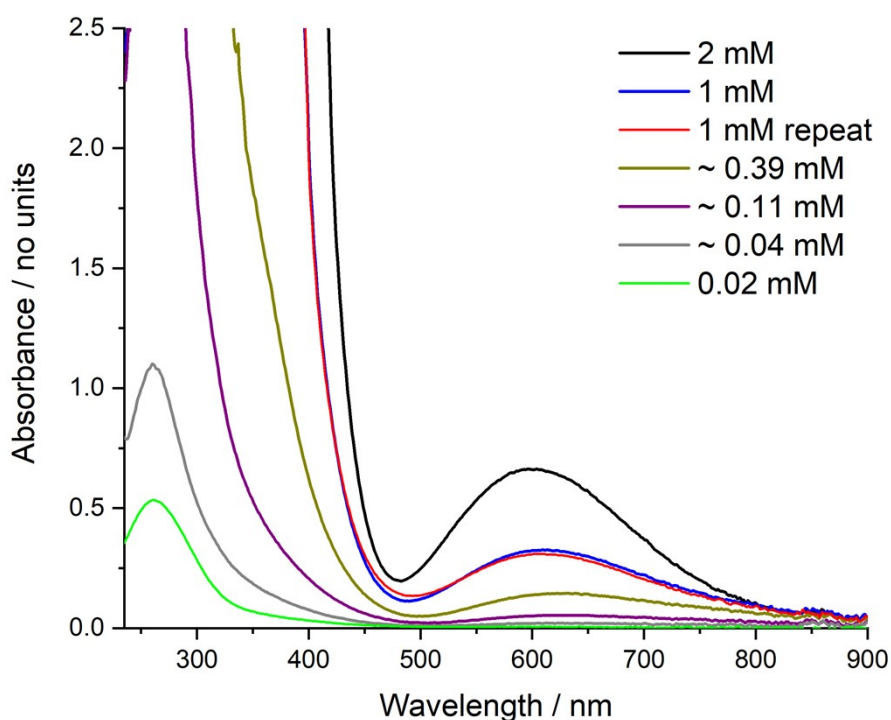


**Figure S28:** UV/vis spectrum of **6** at varying molecular concentrations in  $\text{CH}_2\text{Cl}_2$ . Serial dilutions were inaccurate for the weaker concentrations, therefore approximate concentrations estimated using the Beer-Lambert rule. Spectra were repeated separately for 1 mM and 0.02 mM. Slight shift in absorption is observed around the 450-500 nm area with changing concentration – this may be attributed to different oligomers of  $[\text{Cu}(\text{OEt})(\text{O}_2\text{C}^t\text{Bu})]_n$  (e.g.  $n = 4,6$ )<sup>4</sup> forming concentration dependent equilibria.

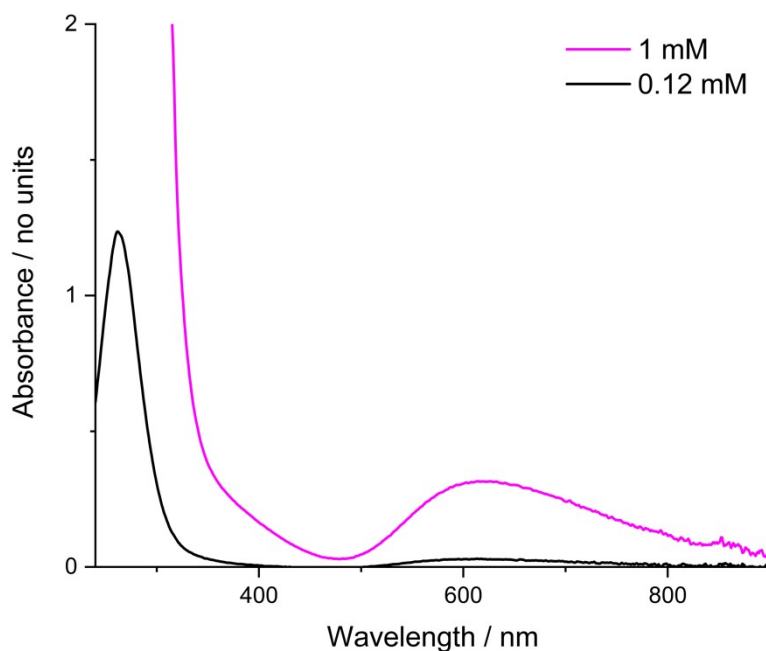


**Figure S29:** UV/vis spectrum of **8** at varying molecular concentrations in  $\text{CH}_2\text{Cl}_2$ .

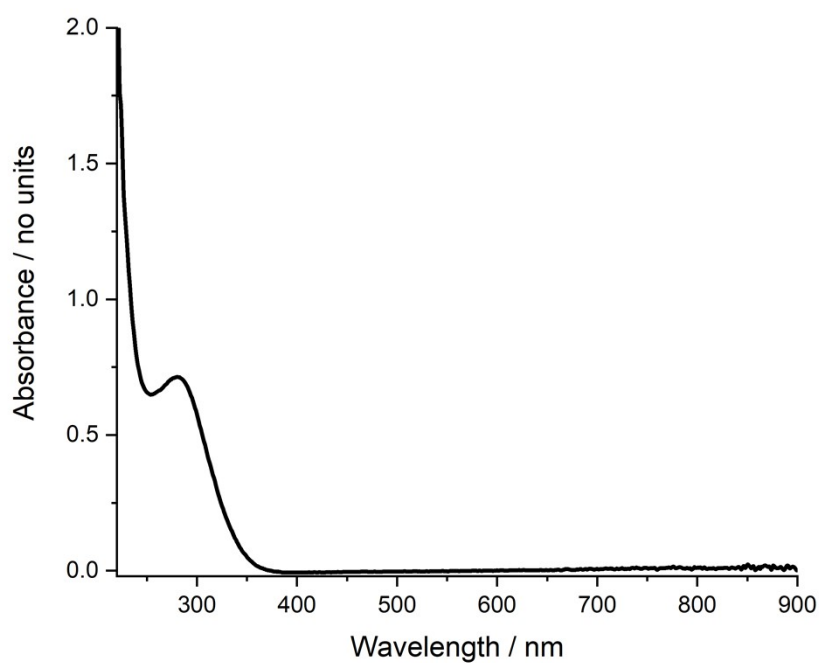


**Figure S30:** UV/vis spectrum of  $\text{Cu}(\text{NO}_3)_2$  (0.4 mM) in  $i\text{PrOH}$ .

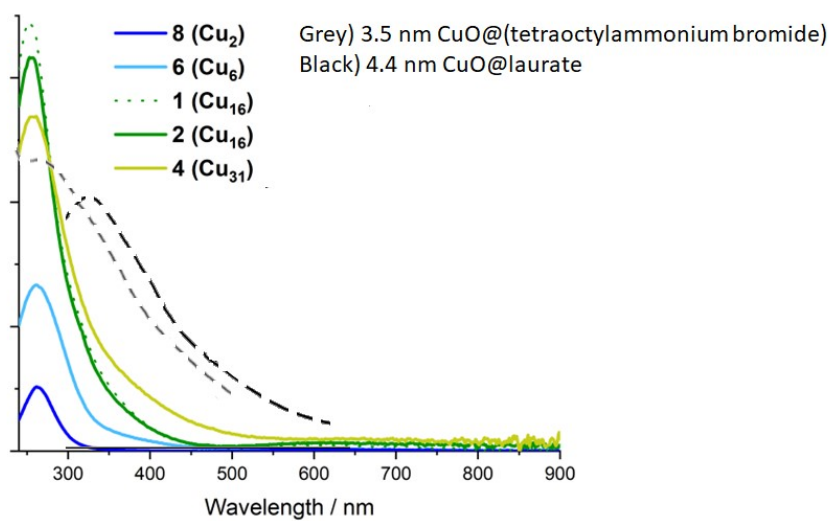


**Figure S31:** UV/vis spectrum of **2**, **4**, **6** and **8** recorded as solutions at 0.1-0.4 mM concentration of Cu ( $\text{mM}[\text{Cu}]$ ) in  $\text{CH}_2\text{Cl}_2$  (or pentane for **2**) in comparison to sketch representing previously reported UV spectra of CuO nanoparticles (arbitrary scale on y-axis).<sup>11, 12</sup>



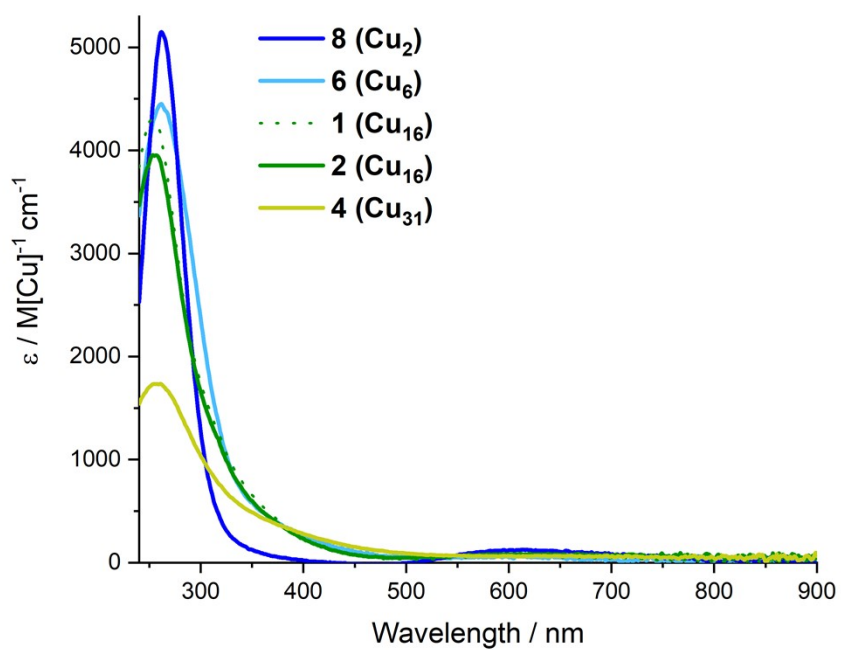


**Figure S32:** UV/vis spectrum of **2**, **4**, **6** and **8** recorded as solutions at 0.1-0.4 mM concentration of Cu (mM[Cu]) in CH<sub>2</sub>Cl<sub>2</sub> (or pentane for **2**), spectra reported as 'per copper' extinction coefficients in mM[Cu]<sup>-1</sup> cm<sup>-1</sup>. Extinction coefficient for **4** with ± 33% error.

O1	OH					O5	H2O							
	r	r0-r	(r0-r)/B	e((r0-r)/B)			r	r0-r	(r0-r)/B	e((r0-r)/B)				
O1-Cu1	2.412	-0.733	-1.9811	0.137920054		O5-Cu7	2.502	-0.823	-2.2243	0.108140462				
O1-Cu3	1.957	-0.278	-0.7514	0.471728651		O5-Cu7	2.502	-0.823	-2.2243	0.108140462				
O1-Cu4	1.953	-0.274	-0.7405	0.476856086		O5-H51	0.955	-0.073	-0.1973	0.820946532				
O1-Cu6	2.696	-1.017	-2.7486	0.064014309		O5-H52	0.956	-0.074	-0.2	0.818730753				
				1.150519099	Good fit for OH					1.855958209	Good fit for H <sub>2</sub> O			
O2	O2-					O13	OH							
	r	r0-r	(r0-r)/B	e((r0-r)/B)			r	r0-r	(r0-r)/B	e((r0-r)/B)				
O2-Cu4	1.961	-0.282	-0.7622	0.466656349		O13-Cu5	1.931	-0.252	-0.6811	0.506069594				
O2-Cu5	1.93	-0.251	-0.6784	0.5074392		O13-Cu5	1.931	-0.252	-0.6811	0.506069594				
O2-Cu6	1.917	-0.238	-0.6432	0.525585057						1.012139189	Good fit for OH			
O2-Cu7	1.911	-0.232	-0.627	0.534177538										
				2.033858143	Good fit for O <sup>2-</sup>	O19	Alkoxide							
O3	O2-						r	r0-r	(r0-r)/B	e((r0-r)/B)				
	r	r0-r	(r0-r)/B	e((r0-r)/B)		O19-Cu3	1.904	-0.225	-0.6081	0.544379803				
O3-Cu3	1.958	-0.279	-0.7541	0.47045543		O19-Cu8	1.908	-0.229	-0.6189	0.538526314				
O3-Cu6	1.913	-0.234	-0.6324	0.531297882		O19-C47	1.415	-0.025	-0.0676	0.934664565				
O3-Cu7	1.922	-0.243	-0.6568	0.51853033						2.017570682	Good fit for alkoxide			
O3-Cu8	1.946	-0.267	-0.7216	0.485963568		O20	Alkoxide							
				2.006247209	Good fit for O <sup>2-</sup>		r	r0-r	(r0-r)/B	e((r0-r)/B)				
O4	OH					O20-Cu1	1.939	-0.26	-0.7027	0.495244993				
	r	r0-r	(r0-r)/B	e((r0-r)/B)		O20-Cu2	1.927	-0.248	-0.6703	0.511570297				
O2-Cu8	1.887	-0.208	-0.5622	0.569975351		O20-Cu3	2.513	-0.834	-2.2541	0.104972795				
O2-Cu8	1.887	-0.208	-0.5622	0.569975351		O20-C49	1.433	-0.043	-0.1162	0.890282709				
				1.139950703	Good fit for OH					2.002070795	Good fit for alkoxide			
O21	Alkoxide					O22	Alkoxide							
	r	r0-r	(r0-r)/B	e((r0-r)/B)			r	r0-r	(r0-r)/B	e((r0-r)/B)				
O21-Cu1	1.94	-0.261	-0.7054	0.493908301		O22-Cu4	1.904	-0.225	-0.6081	0.544379803				
O21-Cu2	1.927	-0.248	-0.6703	0.511570297		O22-Cu5	1.898	-0.219	-0.5919	0.553279549				
O21-Cu4	2.549	-0.87	-2.3514	0.095240372		O22-C53	1.47	-0.08	-0.2162	0.805561108				
O21-C51	1.439	-0.049	-0.1324	0.875962119						1.90322046	Good fit for alkoxide			
				1.976681088	Good fit for alkoxide									

Table S2: Bond valence sum calculations for **3**. For Cu(II)-O,  $r_0 = 1.679$ . For C-O,  $r_0 = 1.39$ . B = 0.37.

**Table S3:** Bond valence sum calculations for **4**. For Cu(II)–O,  $r_0 = 1.679$ . For C–O,  $r_0 = 1.39$ .  $B = 0.37$ .

<b>O1</b>					<b>O6</b>				
r	r0-r	(r0-r)/B	e((ro-r)/B)		r	r0-r	(r0-r)/B	e((ro-r)/B)	
1.9	-0.221	-0.5973	0.55029692		1.975	-0.296	-0.8	0.44932896	
1.91	-0.231	-0.6243	0.53562321		2.035	-0.356	-0.9622	0.3820659	
1.957	-0.278	-0.7514	0.47172865		1.998	-0.319	-0.8622	0.42224813	
1.935	-0.256	-0.6919	0.50062804					1.25364299	<b>Good fit for OH</b>
			2.05827682	<b>Good fit for O<sup>2-</sup></b>					
<b>O2</b>					<b>O7</b>				
r	r0-r	(r0-r)/B	e((ro-r)/B)		r	r0-r	(r0-r)/B	e((ro-r)/B)	
1.914	-0.235	-0.6351	0.52986388		1.983	-0.304	-0.8216	0.43971802	
1.925	-0.246	-0.6649	0.51434303		1.99	-0.311	-0.8405	0.43147723	
2.022	-0.343	-0.927	0.39572845		1.986	-0.307	-0.8297	0.43616715	
1.92	-0.241	-0.6514	0.52134079					1.3073624	<b>Good fit for OH</b>
			1.96127615	<b>Good fit for O<sup>2-</sup></b>					
<b>O3</b>					<b>O8</b>				
r	r0-r	(r0-r)/B	e((ro-r)/B)		r	r0-r	(r0-r)/B	e((ro-r)/B)	
1.913	-0.234	-0.6324	0.53129788		1.921	-0.242	-0.6541	0.51993366	
1.894	-0.215	-0.5811	0.5592934		1.887	-0.208	-0.5622	0.56997535	
1.898	-0.219	-0.5919	0.55327955					1.08990901	<b>Good fit for OH</b>
2.215	-0.536	-1.4486	0.23488749						
			1.87875832	<b>Good fit for O<sup>2-</sup></b>					
<b>O4</b>					<b>O9</b>				
r	r0-r	(r0-r)/B	e((ro-r)/B)		r	r0-r	(r0-r)/B	e((ro-r)/B)	
1.902	-0.223	-0.6027	0.54733036		1.893	-0.214	-0.5784	0.56080705	
1.936	-0.257	-0.6946	0.49927682		1.904	-0.225	-0.6081	0.5443798	
1.904	-0.225	-0.6081	0.5443798		1.947	-0.268	-0.7243	0.48465193	
1.941	-0.262	-0.7081	0.49257522		1.949	-0.27	-0.7297	0.48203925	
			2.0835622	<b>Good fit for O<sup>2-</sup></b>				2.07187803	<b>Good fit for O<sup>2-</sup></b>
<b>O5</b>					<b>O10</b>				
r	r0-r	(r0-r)/B	e((ro-r)/B)		r	r0-r	(r0-r)/B	e((ro-r)/B)	
1.917	-0.238	-0.6432	0.52558506		1.999	-0.32	-0.8649	0.42110846	
1.902	-0.223	-0.6027	0.54733036		2.008	-0.329	-0.8892	0.41098885	
			1.07291542	<b>Good fit for OH</b>	2.011	-0.332	-0.8973	0.40766998	
								1.23976729	<b>Good fit for OH</b>

O11			
r	r0-r	(r0-r)/B	e((ro-r)/B)
1.911	-0.232	-0.627	0.53417754
1.924	-0.245	-0.6622	0.51573503
			1.04991256

Good fit for OH

O181			
r	r0-r	(r0-r)/B	e((ro-r)/B)
2.331	-0.652	-1.7622	0.17167328
1.499	-0.109	-0.2946	0.74483349
			0.91650676

Good fit for alcohol

O12			
r	r0-r	(r0-r)/B	e((ro-r)/B)
1.99	-0.311	-0.8405	0.43147723
1.998	-0.319	-0.8622	0.42224813
2.019	-0.34	-0.9189	0.39895011
			1.25267546

Good fit for OH

O39			
r	r0-r	(r0-r)/B	e((ro-r)/B)
0.944	-0.062	-0.1676	0.84571947
1.457	-0.067	-0.1811	0.8343677
			1.68008718

Free alcohol

O13			
r	r0-r	(r0-r)/B	e((ro-r)/B)
1.984	-0.305	-0.8243	0.4385312
1.986	-0.307	-0.8297	0.43616715
1.984	-0.305	-0.8243	0.4385312
			1.31322955

Good fit for OH

O170			
r	r0-r	(r0-r)/B	e((ro-r)/B)
2.347	-0.668	-1.8054	0.16440779
1.424	-0.034	-0.0919	0.91220376
			1.07661155

Good fit for alcohol

O14			
r	r0-r	(r0-r)/B	e((ro-r)/B)
2.072	-0.393	-1.0622	0.34570753
1.899	-0.22	-0.5946	0.55178622
1.933	-0.254	-0.6865	0.50334146
1.916	-0.237	-0.6405	0.52700748
			1.92784268

Good fit for O<sup>2-</sup>

O40			
r	r0-r	(r0-r)/B	e((ro-r)/B)
0.951	-0.069	-0.1865	0.82986978
1.467	-0.077	-0.2081	0.81211924
			1.64198901

Free alcohol

O29			
r	r0-r	(r0-r)/B	e((ro-r)/B)
1.974	-0.295	-0.7973	0.45054501
1.985	-0.306	-0.827	0.43734758
1.986	-0.307	-0.8297	0.43616715
			1.32405974

Good fit for OH

O151			
r	r0-r	(r0-r)/B	e((ro-r)/B)
2.325	-0.646	-1.7459	0.17447986
1.444	-0.054	-0.1459	0.86420442
			1.03868428

Good fit for alcohol

**Table S4:** Bond valence sum calculations for 5. For Cu(II)–O,  $r_0 = 1.679$ . For C–O,  $r_0 = 1.39$ .  $B = 0.37$ .

<b>O1</b>	<b>OH</b>								
	r	r0-r	(r0-r)/B	e((r0-r)/B)					
O1-Cu1	1.978	-0.299	-0.8081	0.4457					
O1-Cu2	2.002	-0.323	-0.873	0.4177					
O1-Cu4	2.01	-0.331	-0.8946	0.4088					
				1.2722	<b>Good fit for OH</b>				
<b>O2</b>	<b>OH</b>								
	r	r0-r	(r0-r)/B	e((r0-r)/B)					
O2-Cu2	1.911	-0.232	-0.627	0.5342					
O2-Cu6	1.924	-0.245	-0.6622	0.5157					
				1.0499	<b>Good fit for OH</b>				
<b>O3</b>	<b>OH</b>								
	r	r0-r	(r0-r)/B	e((r0-r)/B)					
O3-Cu1	1.979	-0.3	-0.8108	0.4445					
O3-Cu4	2.004	-0.325	-0.8784	0.4155					
O3-Cu5	2.002	-0.323	-0.873	0.4177					
				1.2777	<b>Good fit for OH</b>				
<b>O4</b>	<b>O2-</b>								
	r	r0-r	(r0-r)/B	e((r0-r)/B)					
O4-Cu2	1.94	-0.261	-0.7054	0.4939					
O4-Cu3	1.898	-0.219	-0.5919	0.5533					
O4-Cu6	1.949	-0.27	-0.7297	0.482					
O4-Cu7	1.906	-0.227	-0.6135	0.5414					
				2.0707	<b>Good fit for O<sup>2-</sup></b>				
<b>O5</b>	<b>O2-</b>								
	r	r0-r	(r0-r)/B	e((r0-r)/B)					
O5-Cu5	1.949	-0.27	-0.7297	0.482					
O5-Cu7	1.907	-0.228	-0.6162	0.54					
O5-Cu8	1.95	-0.271	-0.7324	0.4807					
O5-Cu10	1.903	-0.224	-0.6054	0.5459					
				2.0486	<b>Good fit for O<sup>2-</sup></b>				
<b>O6</b>	<b>O2-</b>								
	r	r0-r	(r0-r)/B	e((r0-r)/B)					
O6-Cu7	1.907	-0.228	-0.6162	0.54					
O6-Cu9	1.898	-0.219	-0.5919	0.5533					
O6-Cu11	2.368	-0.689	-1.8622	0.1553					
O6-Cu14	1.892	-0.213	-0.5757	0.5623					
				1.8109	<b>Good fit for O<sup>2-</sup></b>				
<b>O7</b>	<b>O2-</b>								
	r	r0-r	(r0-r)/B	e((r0-r)/B)					
O7-Cu3	1.908	-0.229	-0.6189	0.538526314					
O7-Cu4	1.924	-0.245	-0.6622	0.515735025					
O7-Cu11	1.98	-0.301	-0.8135	0.443297794					
O7-Cu14	1.938	-0.259	-0.7	0.496585304					
				1.994144437	<b>Good fit for O<sup>2-</sup></b>				
<b>O8</b>	<b>OH</b>								
	r	r0-r	(r0-r)/B	e((r0-r)/B)					
O8-Cu8	1.981	-0.302	-0.8162	0.442101309					
O8-Cu14	2.002	-0.323	-0.873	0.417707867					
O8-Cu16	1.969	-0.29	-0.7838	0.456674779					
				1.316483956	<b>Good fit for OH</b>				
<b>O9</b>	<b>O2-</b>								
	r	r0-r	(r0-r)/B	e((r0-r)/B)					
O9-Cu4	1.928	-0.249	-0.673	0.510189541					
O9-Cu9	1.93	-0.251	-0.6784	0.5074392					
O4-Cu10	1.908	-0.229	-0.6189	0.538526314					
O4-Cu11	2.006	-0.327	-0.8838	0.413216428					
				1.969371483	<b>Good fit for O<sup>2-</sup></b>				
<b>O10</b>	<b>O2-</b>								
	r	r0-r	(r0-r)/B	e((r0-r)/B)					
O10-Cu3	1.89	-0.211	-0.5703	0.565372615					
O10-Cu1	1.898	-0.219	-0.5919	0.553279549					
O10-Cu1	1.94	-0.261	-0.7054	0.493908301					
O10-Cu1	1.942	-0.263	-0.7108	0.491245729					
				2.103806193	<b>Good fit for O<sup>2-</sup></b>				
<b>O11</b>	<b>OH</b>								
	r	r0-r	(r0-r)/B	e((r0-r)/B)					
O11-Cu9	2.036	-0.357	-0.9649	0.381034687					
O11-Cu1	1.996	-0.317	-0.8568	0.424536728					
O11-Cu1	1.997	-0.318	-0.8595	0.42339088					
				1.228962296	<b>Good fit for OH</b>				
<b>O12</b>	<b>OH</b>								
	r	r0-r	(r0-r)/B	e((r0-r)/B)					
O12-Cu6	1.991	-0.312	-0.8432	0.430312649					
O12-Cu9	1.989	-0.31	-0.8378	0.432644961					
O12-Cu1	1.968	-0.289	-0.7811	0.457910705					
				1.320868316	<b>Good fit for OH</b>				

O37	r	r0-r	(r0-r)/B	e((r0-r)/B)		O38	r	r0-r	(r0-r)/B	e((r0-r)/B)	
O37-Cu1	2.291	-0.612	-1.6541	0.191272904	Good fit for CypOH	O38-Cu1	2.287	-0.608	-1.6432	0.193351937	Good fit for CypOH
O37-C56	1.448	-0.058	-0.1568	0.854911985		O38-C51	1.423	-0.033	-0.0892	0.914672511	
				1.046184889						1.108024448	
O42	r	r0-r	(r0-r)/B	e((r0-r)/B)		O39	r	r0-r	(r0-r)/B	e((r0-r)/B)	
O42-C71	1.492	-0.102	-0.2757	0.759059072	Free CypOH	O39-Cu1	2.298	-0.619	-1.673	0.187688243	Good fit for CypOH
O42-H42	0.949	-0.067	-0.1811	0.834367705		O39-C46	1.448	-0.058	-0.1568	0.854911985	
				1.593426777						1.042600228	
O43	r	r0-r	(r0-r)/B	e((r0-r)/B)							
O43-C86	1.472	-0.082	-0.2216	0.801218471	Free CypOH						
O43-H43	0.95	-0.068	-0.1838	0.832115701							
				1.633334172							

**Table S5:** Bond valence sum calculations for **6**. For Cu(II)-O,  $r_0 = 1.679$ . For C-O,  $r_0 = 1.39$ .  $B = 0.37$ .

O13	r	r0-r	(r0-r)/B	e((r0-r)/B)		O16	r	r0-r	(r0-r)/B	e((r0-r)/B)	
O13-Cu2	1.91	-0.231	-0.6243243	0.53562321	Good fit for alkoxide	O16-Cu1	1.906	-0.227	-0.6135135	0.54144515	Good fit for alkoxide
O13-Cu3	1.905	-0.226	-0.6108108	0.54291049		O16-Cu6	1.915	-0.236	-0.6378378	0.52843375	
O13-C31	1.422	0.032	0.08648649	1.09033663		O16-C37	1.423	-0.033	-0.0891892	0.91467251	
				2.16887034						1.98455141	
O14	r	r0-r	(r0-r)/B	e((r0-r)/B)		O17	r	r0-r	(r0-r)/B	e((r0-r)/B)	
O14-Cu2	1.9	-0.221	-0.5972973	0.55029692	Good fit for alkoxide	O17-Cu4	1.907	-0.228	-0.6162162	0.53998376	Good fit for alkoxide
O14-Cu3	1.91	-0.231	-0.6243243	0.53562321		O17-Cu5	1.902	-0.223	-0.6027027	0.54733036	
O14-C33	1.422	-0.032	-0.0864865	0.91714794		O17-C39	1.424	-0.034	-0.0918919	0.91220376	
				2.00306807						1.99951788	
O15	r	r0-r	(r0-r)/B	e((r0-r)/B)		O18	r	r0-r	(r0-r)/B	e((r0-r)/B)	
O15-Cu1	1.906	-0.227	-0.6135135	0.54144515	Good fit for alkoxide	O18-Cu4	1.908	-0.229	-0.6189189	0.53852631	Good fit for alkoxide
O15-Cu6	1.903	-0.224	-0.6054054	0.54585309		O18-Cu5	1.907	-0.228	-0.6162162	0.53998376	
O15-C35	1.419	-0.029	-0.0783784	0.92461451		O18-C41	1.42	-0.03	-0.0810811	0.92211892	
				2.01191274						2.00062899	

**Table S6:** Bond valence sum calculations for **7**. For Cu(II)-O,  $r_0 = 1.679$ . For C-O,  $r_0 = 1.39$ .  $B = 0.37$ .

<b>O1</b>							<b>O6</b>					
	r	r0-r	(r0-r)/B	e((r0-r)/B)				r	r0-r	(r0-r)/B	e((r0-r)/B)	
O1-Cu1	2.003	-0.324	-0.8757	0.416580451			O6-Cu2	1.978	-0.299	-0.8081	0.445700486	
O1-Cu2	2.002	-0.323	-0.873	0.417707867			O6-Cu5	1.981	-0.302	-0.8162	0.442101309	
O1-Cu3	2.263	-0.584	-1.5784	0.206309383			O6-Cu6	1.989	-0.31	-0.8378	0.432644961	
O1-Cu4	2.001	-0.322	-0.8703	0.418838334						1.320446757	Good fit for OH	
O1-Cu11	2.007	-0.328	-0.8865	0.412101135			<b>O7</b>					
				1.871537171	Good fit for O <sup>2-</sup>			r	r0-r	(r0-r)/B	e((r0-r)/B)	
<b>O2</b>							O7-Cu2	1.986	-0.307	-0.8297	0.436167153	
	r	r0-r	(r0-r)/B	e((r0-r)/B)			O7-Cu6	1.989	-0.31	-0.8378	0.432644961	
O2-Cu3	1.893	-0.214	-0.5784	0.560807046			O7-Cu7	1.988	-0.309	-0.8351	0.433815854	
O2-Cu11	1.872	-0.193	-0.5216	0.593557242						1.302627969	Good fit for OH	
O2-Cu12	1.941	-0.262	-0.7081	0.492575216			<b>O8</b>					
O2-Cu15	1.949	-0.27	-0.7297	0.482039253				r	r0-r	(r0-r)/B	e((r0-r)/B)	
				2.128978757	Good fit for O <sup>2-</sup>		O8-Cu2	1.975	-0.299	-0.8081	0.44570049	
<b>O3</b>							O8-Cu10	1.983	-0.302	-0.8162	0.44210131	
	r	r0-r	(r0-r)/B	e((r0-r)/B)			O8-Cu12	1.984	-0.31	-0.8378	0.43264496	
O3-Cu3	1.894	-0.215	-0.5811	0.559293398						1.32044676	Good fit for OH	
O3-Cu4	1.881	-0.202	-0.5459	0.579293544			<b>O9</b>					
O3-Cu7	1.93	-0.251	-0.6784	0.5074392				r	r0-r	(r0-r)/B	e((r0-r)/B)	
O3-Cu8	1.947	-0.268	-0.7243	0.484651926			O9-Cu2	1.979	-0.3	-0.8081	0.44570049	
				2.130678068	Good fit for O <sup>2-</sup>		O9-Cu10	1.988	-0.309	-0.8162	0.44210131	
<b>O4</b>							O2-Cu13	1.99	-0.311	-0.8378	0.43264496	
	r	r0-r	(r0-r)/B	e((r0-r)/B)						1.32044676	Good fit for OH	
O4-Cu1	1.893	-0.214	-0.5784	0.560807046			<b>O18</b>					
O4-Cu4	1.886	-0.207	-0.5595	0.571517909				r	r0-r	(r0-r)/B	e((r0-r)/B)	
O4-Cu5	1.925	-0.246	-0.6649	0.514343029			O18-Cu9	1.924	-0.245	-0.6622	0.515735025	
O4-Cu9	1.938	-0.259	-0.7	0.496585304			O18-Cu17	1.936	-0.257	-0.6946	0.499276816	
				2.143253288	Good fit for O <sup>2-</sup>		O18-C480	1.335	0.055	0.1486	1.160265257	
<b>O5</b>										2.175277099	Good fit for alkoxide	
	r	r0-r	(r0-r)/B	e((r0-r)/B)			<b>O19</b>					
O5-Cu1	1.892	-0.213	-0.5757	0.562324791				r	r0-r	(r0-r)/B	e((r0-r)/B)	
O5-Cu11	1.882	-0.203	-0.5486	0.577729999			O19-Cu8	1.934	-0.255	-0.6892	0.501982917	
O5-Cu13	1.935	-0.256	-0.6919	0.500628038			O19-Cu17	1.926	-0.247	-0.6676	0.512954789	
O5-Cu14	1.945	-0.266	-0.7189	0.487278759			O19-C511	1.351	0.039	0.1054	1.11116099	
				2.127961588	Good fit for O <sup>2-</sup>					2.126098696	Good fit for alkoxide	



<b>O20</b>				
	r	r0-r	(r0-r)/B	e((r0-r)/B)
O20-Cu14	1.942	-0.263	-0.7108	0.491245729
O20-Cu16	1.942	-0.263	-0.7108	0.491245729
O20-C590	1.389	0.001	0.0027	1.002706358
				1.985197815

Good fit for alkoxide

<b>O36</b>				
	r	r0-r	(r0-r)/B	e((r0-r)/B)
O36-Cu7	1.916	-0.237	-0.6405	0.527007478
O36-Cu8	1.923	-0.244	-0.6595	0.517130789
O36-C37	1.443	-0.053	-0.1432	0.866543262
				1.91068153

Good fit for alkoxide

<b>O21</b>				
	r	r0-r	(r0-r)/B	e((r0-r)/B)
O21-Cu15	1.934	-0.255	-0.6892	0.501982917
O21-Cu16	1.942	-0.263	-0.7108	0.491245729
O21-C621	1.427	-0.037	-0.1	0.904837418
				1.898066064

Good fit for alkoxide

<b>O37</b>				
	r	r0-r	(r0-r)/B	e((r0-r)/B)
O37-Cu12	1.908	-0.229	-0.6189	0.538526314
O37-Cu15	1.916	-0.237	-0.6405	0.527007478
O37-C40	1.433	-0.043	-0.1162	0.890282709
				1.955816501

Good fit for alkoxide

<b>O32</b>				
	r	r0-r	(r0-r)/B	e((r0-r)/B)
O32-Cu5	1.911	-0.232	-0.627	0.534177538
O32-Cu9	1.926	-0.247	-0.6676	0.512954789
O32-C11	1.435	-0.045	-0.1216	0.885483353
				1.93261568

Good fit for alkoxide

<b>O37</b>				
	r	r0-r	(r0-r)/B	e((r0-r)/B)
O37-Cu12	1.908	-0.229	-0.6189	0.538526314
O37-Cu15	1.916	-0.237	-0.6405	0.527007478
O37-C40	1.433	-0.043	-0.1162	0.890282709
				1.955816501

Good fit for alkoxide

<b>O35</b>				
	r	r0-r	(r0-r)/B	e((r0-r)/B)
O35-Cu13	1.913	-0.234	-0.6324	0.531297882
O35-Cu14	1.937	-0.258	-0.6973	0.497929242
O35-C14	1.428	-0.038	-0.1027	0.902395213
				1.931622337

Good fit for alkoxide

## Crystallography Tables

Compound	<b>3</b>	<b>4</b>	<b>5</b>
CCDC No.	2211399	2211400	2211401
Formula	C <sub>81</sub> H <sub>180</sub> Cu <sub>16</sub> O <sub>41</sub>	C <sub>126</sub> H <sub>276</sub> Cu <sub>31</sub> N <sub>2</sub> O <sub>84</sub>	C <sub>150</sub> H <sub>300</sub> Cu <sub>31</sub> N <sub>2</sub> O <sub>84</sub>
M	2827	5133	5446
Crystal System	Monoclinic	Monoclinic	Monoclinic
Space group	P 2 <sub>1</sub> /m	P 2 <sub>1</sub> /n	P 2 <sub>1</sub> /n
T [K]	100	100	100
a [Å]	14.4485(3)	19.2171(6)	19.41100(10)
b [Å]	22.5228(4)	19.0958(6)	21.32210(10)
c [Å]	18.5406(4)	26.9688(8)	28.21580
α [deg]	90	90	90
β [deg]	96.0323(18)	90.3848(17)	92.1343
γ [deg]	90	90	90
V [Å <sup>3</sup> ]	6000.1(2)	9896.4(3)	11669.95(9)
Z	2	2	4
θ range [deg]	3.076 – 80.020	2.814 – 67.167	3.12 – 78.27
Reflns collected	88854	130526	107115
R int	0.064	0.125	0.033
No. of data/restr/param	13091/2204/828	17551/1952/1420	24720/180/1412
R <sub>1</sub> [I>2σ(I)]	0.0796	0.1166	0.0426
wR <sub>2</sub> [all data]	0.1797	0.2273	0.1263
GoF	1.0068	1.0072	0.9958
Largest diff. pk and hole [eÅ <sup>3</sup> ]	-1.26, 1.34	-1.42, 1.71	-1.10, 1.60

Compound	<b>6</b>	<b>7</b>	<b>8</b>
CCDC No.	2211402	2211403	2220157
Formula	C <sub>42</sub> H <sub>84</sub> Cu <sub>6</sub> O <sub>18</sub>	C <sub>80</sub> H <sub>170</sub> Cu <sub>17</sub> N <sub>6</sub> O <sub>49</sub>	C <sub>26</sub> H <sub>54</sub> Cu <sub>2</sub> O <sub>11</sub>
M	1258.39	3080.52	669.80
Crystal System	Monoclinic	Monoclinic	Triclinic
Space group	P 2 <sub>1</sub> /c	P 2 <sub>1</sub> /n	P -1
T [K]	100	100	100
a [Å]	14.57980(10)	19.35030(10)	11.57930(10)
b [Å]	15.13330(10)	33.6673(3)	11.94480(10)
c [Å]	28.5685(2)	21.1824(2)	14.63380(10)
α [deg]	90	90	99.4804(8)
β [deg]	102.2096(8)	95.7608(7)	110.8148(8)
γ [deg]	90	90	105.8283(3)
V [Å <sup>3</sup> ]	6160.79(8)	13730.05(19)	1741.46(3)
Z	4	1	2
θ range [deg]	3.101 – 79.994	3.228 – 80.548	3.377 – 77.014
Reflns collected	147889	137951	51706
R int	0.064	0.050	0.056
No. of data/restr/param	13310/0/658	29195/1523/1630	7009/632/473
R <sub>1</sub> [I>2σ(I)]	0.0310	0.0552	0.0498
wR <sub>2</sub> [all data]	0.0911	0.1611	0.1292
GoF	1.0086	1.0000	1.0098
Largest diff. pk and hole [eÅ <sup>3</sup> ]	-0.63, 0.41	-1.18, 2.12	-1.29, 1.26

## References

1. Bruker (2001). SADABS. Bruker AXS Inc., Madison, Wisconsin, USA.
2. Palatinus, L.; Chapuis, G., *J. Appl. Crystallogr.* **2007**, *40* (4), 786-790.
3. Betteridge, P. W.; Carruthers, J. R.; Cooper, R. I.; Prout, K.; Watkin, D. J., *J. Appl. Crystallogr.* **2003**, *36* (6), 1487.
4. Liu, T.-F.; Stamatatos, T. C.; Abboud, K. A.; Christou, G., *Dalton Trans.* **2010**, *39* (15), 3554-3556.
5. Singh, J. V.; Baranwal, B. P.; Mehrotra, R. C., *Z. Anorg. Allg. Chem.* **1981**, *477* (6), 235-240.
6. Zhou, J.-H.; Liu, Z.; Li, Y.-Z.; Song, Y.; Chen, X.-T.; You, X.-Z., *J. Coord. Chem.* **2006**, *59* (2), 147-156.
7. Liu, B., *Nanoscale* **2012**, *4* (22), 7194-7198.
8. Masahiro, M.; Hiroshi, A.; Ryoji, N.; Makoto, H., *Chem. Lett.* **1999**, *28* (1), 57-58.
9. Li, R.; Greaves, C., *J. Solid State Chem.* **2020**, *291*, 121612.
10. Pike, S. D.; White, E. R.; Regoutz, A.; Sammy, N.; Payne, D. J.; Williams, C. K.; Shaffer, M. S. P., *ACS Nano* **2017**, *11* (3), 2714-2723.
11. Estruga, M.; Roig, A.; Domingo, C.; Ayllón, J. A., *J. Nanopart. Res.* **2012**, *14* (8), 1053.
12. Borgohain, K.; Mahamuni, S., *J. Mater. Res.* **2002**, *17* (5), 1220-1223.